Electronic Supplementary Material (ESI) for Physical Chemistry Chemical Physics.
This journal is © the Owner Societies 2023

Supporting Information for

Bounding $[AnO_2]^{2+}$ (An=U, Np) covalency by simulated O K-edge and An M-edge X-ray absorption near-edge spectroscopy

Kurtis Stanistreet-Welsh[a] and Andrew Kerridge[*a]

[a] Department of Chemistry, Lancaster University, Lancaster LA1 4YB, UK

Table of Contents:

1. Computational Details:

1.1 General Comment:

Unless stated otherwise, all spectra in this supporting document are unshifted, meaning energies (eV) are those taken directly from RASSI calculations. All theoretical XANES curves are generated from fitting Lorentzian functions across all intense states with a full-width at half-maximum value of 0.80 eV and 1.00 eV for ligand- and metal-edge XANES simulations respectively.

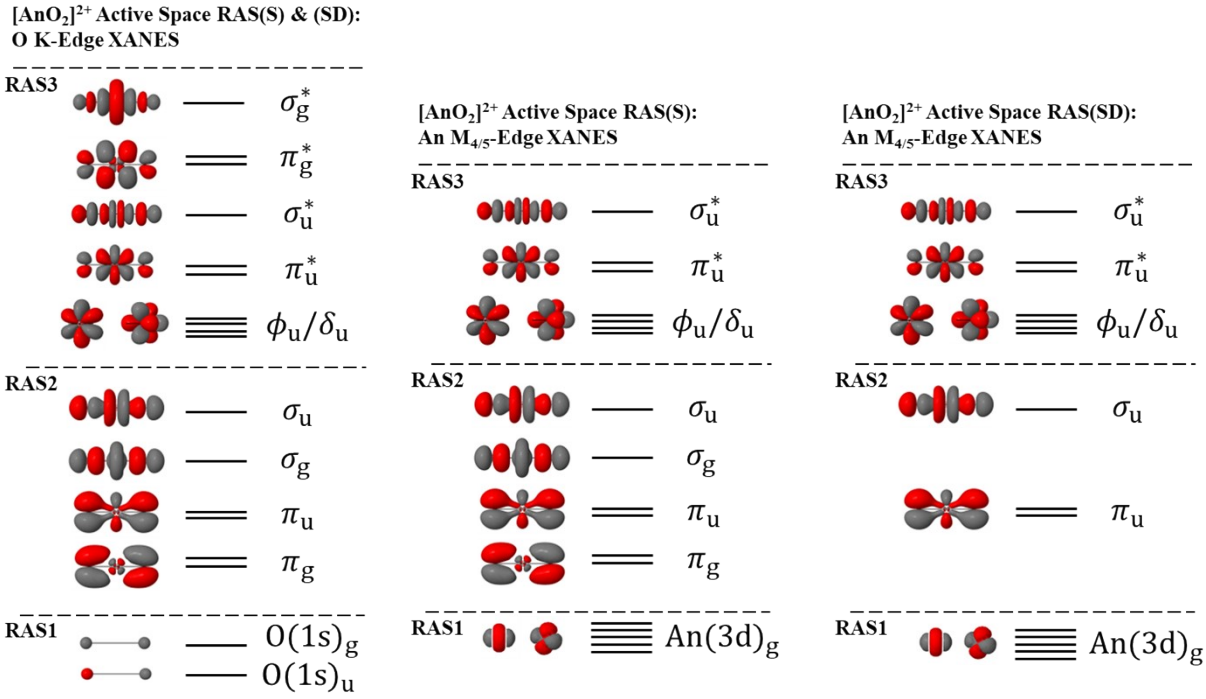

Figure S1: Active spaces for XANES RASSCF simulations.

1.2 Ground-states for both O K-Edge and An $M_{4/5}$-Edge XANES:

Ground-states were obtained through state-averaging, which was found to stabilize the active-spaces. The $[UO_2]^{2+}$ ground-state, $\Psi_{GS} = {}^1(A_g)_1$, is obtained by taking the first root of the Ag singlet wavefunctions in both ligand- and metal-edge simulations. The $[NpO_2]^{2+}$ ground-state takes the form of a degenerate pair of Kramers doublets (a result of the half-integer total spin) and are obtained via a spin-orbit coupling of the first roots of the four spin-free RASSCF ungerade (u) irreducible representations of the doublet wavefunctions. These spin-free states represent the four possible ways of arranging a single electron across the set of non-bonding 5f orbitals. The $[NpO_2]^{2+}$ spin-orbit coupled ground-state in both the degenerate Kramers pair for O K-edge RAS(SD) XANES can be expressed as:

$$\Psi_{GS} = 0.4451^2(B_{2u})_1 + 0.4438^2(B_{3u})_1 + 0.0562^2(B_{1u})_1 + 0.055^2(A_u)_1$$

The $[NpO_2]^{2+}$ spin-orbit coupled ground-state in both the degenerate Kramers pair for Np $M_{4/5}$-Edge RAS(S) XANES can be expressed as:

$$\Psi_{GS} = 0.4305^2(B_{2u})_1 + 0.4294^2(B_{3u})_1 + 0.0708^2(B_{1u})_1 + 0.0693^2(A_u)_1$$

with weights taken from RASSI calculations.

1.3 Additional Considerations for O K-Edge XANES Simulations:

The active space for both $[AnO_2]^{2+}$ systems (figure S1) comprise the occupied linear combination of oxygen 1s orbitals in RAS1 (2 orbitals), the occupied valence bonding orbitals in RAS2 (6 orbitals), and the formally non-bonding 5f orbitals and empty anti-bonding orbitals in RAS3 (10 orbitals). For $[UO_2]^{2+}$, RAS(S) and RAS(SD) wavefunctions are generated by allowing up to 1 or 2 electrons across RAS3 respectively. For $[NpO_2]^{2+}$, RAS3 is allowed up to 2 or 3 electrons for RAS(S) and RAS(SD) wavefunctions respectively, set in order to account for the single unpaired 5f electron. For $[UO_2]^{2+}$ both the non-bonding and anti-bonding orbitals are vacant of electrons in the GS and the RAS3 space reflects this. $[NpO_2]^{2+}$ also has an empty set

of anti-bonding orbitals in the GS but contains a single unpaired electron across the non-bonding 5f orbitals. To generate core-excited states at both the RAS(S) and RAS(SD) levels, a single core-hole is enforced across RAS1 for both systems usings the HEXS keyword. Core-excitations for $[UO_2]^{2+}$ can take the form of singlet or triplet wavefunctions depending on the spin-alignments of electrons. Both the singlet ground-state, and set of singlet and triplet core-ESs, are spin-orbit coupled through the RASSI module. $[NpO_2]^{2+}$ core-excitations take the form of doublet or quartet wavefunctions, which are spin-orbit coupled through the RASSI module along with the first roots of A_u, B_{1u}, B_{2u} and B_{3u} symmetry which couple to generate the $[NpO_2]^{2+}$ degenerate Kramer ground-states. In both cases, the resulting spin-orbit coupled energies (converted to electron-volts) and dipole-oscillator strengths between the core-states and the ground-states are plotted to generate the various O K-Edge XANES transition sticks. For $[NpO_2]^{2+}$, both the degenerate Kramer ground-states and their dipole-oscillator strengths with the various core-ESs are plotted as transition sticks and contribute to the overall XANES curve. Lorentzian functions are fitted to all intense states using a full-width at half maximum (FWHM) value of 0.80 eV, to generate the overall XANES curves for RAS(S) and RAS(SD) simulations.

Tables S1-7 show the number of RASSCF state-averages performed out of the total number of theoretically possible core-states. Tables also report the number roots from these state-averages that went on to be used in state-interaction calculations (RASSI). At the RAS(SD) level of theory, the Laporte selection rule for centrosymmetric systems is applied to reduce the number of states supplied to the state-interaction calculation. Which aids in reducing computational cost. Making use of this selection rule is shown to be valid by comparing the generated spectra of both $[UO_2]^{2+}$ and $[NpO_2]^{2+}$ with and without applying the selection rule when choosing which states were included in RASSI calculations. The results of which are shown in figure S3 and indicate that the selection rule has no notable effect on the spectrum generated. Additionally, at the RAS(SD) level of calculation, maximum energy cutoffs were also used to inform which spin-free states would be included in RASSI calculations, these were 553eV and 547eV cutoffs for $[UO_2]^{2+}$ and $[NpO_2]^{2+}$ states respectively. Values were chosen with the desired goal of restricting the final spectrum to the 525-545eV energy range and to reduce the number of states supplied to RASSI to reduce computational cost.

1.4 Additional Considerations for An $M_{4/5}$-Edge XANES simulations:

The active space for both $[AnO_2]^{2+}$ systems (figure S1) at the RAS(S) level of theory comprise the occupied set of metal core 3d orbitals in RAS1 (5 orbitals), the full set of valence bonding orbitals in RAS2 (6 orbitals), and only the ungerade set of anti-bonding orbitals and non-bonding 5f-orbitals in RAS3 (7 orbitals). At the higher RAS(SD) level of theory, the RAS2 set of orbitals is reduced (3 orbitals) to comprise only those bonding orbitals that pair with the anti-bonding set in RAS3. This was done to reduce computational cost and the simulation results are those presented in the main text. The active space is set-up such that it will fulfill the Laporte selection rule, with the set of 3d orbitals spanning the gerade irreps and the anti-bonding orbitals of interest spanning the ungerade irreps, thus capturing the expected core-excitations responsible for the $M_{4/5}$-edge spectra.

For $[UO_2]^{2+}$, RAS(S) and RAS(SD) wavefunctions are generated by allowing up to 1 or 2 electrons across RAS3 respectively. For $[NpO_2]^{2+}$, RAS3 is allowed up to 2 or 3 electrons for RAS(S) and RAS(SD) wavefunctions respectively, set in order to account for the single unpaired 5f electron. For $[UO_2]^{2+}$ both the non-bonding and anti-bonding orbitals are vacant of electrons in the GS and the RAS3 space reflects this. $[NpO_2]^{2+}$ also has an empty set of anti-bonding orbitals in the GS but contains a single unpaired electron across the non-bonding 5f orbitals. At the RAS(S) and RAS(SD) levels of theory, a single core-hole is enforced across RAS1. To generate core-excited states at both the RAS(S) and RAS(SD) levels, a single core-hole is enforced across RAS1 for both systems usings the HEXS keyword. Core-excitations for $[UO_2]^{2+}$ can take the form of singlet or triplet wavefunctions depending on the spin-alignments of electrons. Both the singlet ground-state, and set of singlet and triplet core-ESs, are spin-orbit coupled through the RASSI module. $[NpO_2]^{2+}$ core-excitations take the form of doublet or quartet wavefunctions, which are spin-orbit coupled through the RASSI module, along with the first roots of A_u, B_{1u}, B_{2u} and B_{3u} ground-states which couple to generate the $[NpO_2]^{2+}$ degenerate Kramer ground-states. In both cases, the resulting spin-orbit coupled energies (converted to electron-volts) and dipole-oscillator strengths between the core-states and the ground-states are plotted to generate the various An $M_{4/5}$-Edge XANES transition sticks. For $[NpO_2]^{2+}$, both degenerate Kramer ground-states and their dipole-oscillator strengths with the various core-ESs are plotted as transition sticks and contribute to the overall XANES curves. Lorentzian functions are fitted to all intense states with a full-width at half maximum (FWHM) value of 1.00 eV utilized to generate the overall XANES curves for RAS(S) simulations.

Tables S1-7 show the number of RASSCF state-averages actually performed out of the total number of theoretically possible core-states and further reports the number roots from these state-averages that went on to be used in state-interaction calculations. To reduce the computational cost of state-interaction calculations, spin-free spectra for both systems at the RAS(S) level of theory, figure S2, were utilized to inform a maximum energy cutoff for spin-free states supplied to RASSI calculations at the RAS(SD) level. Energy cutoffs of 3657 eV and 3773 eV were chosen for M_4-edge for $[UO_2]^{2+}$ and M_5-edge for $[NpO_2]^{2+}$. Figure S4, shows the validity of this approach, as the RAS(S) M_5-edge spectra for $[NpO_2]^{2+}$ when including all possible core-ESs and when reducing the number of states according to the energy cutoff, both generate

spectra that are qualitatively identical. Thus, the same energy cutoffs were used to inform the size of production level RASSI calculations.

2. Number of State-Averages Performed & States Included in RASSI Calculations:

Table S1: Number of state-average RASSCF roots and states used in subsequent RASSI calculations for RAS(S) O K-edge $[UO_2]^{2+}$ XANES simulations. States in bold are those used when the Laporte selection rule was imposed. GS = Ground-State, Core-ES = Core-Excited State.

	AG	B1G	B2G	B3G	AU	B1U	B2U	B3U
GS Singlet								
State-Average Performed:	3							
Used in RASSI:	**1**							
Core-ES Singlets								
State-Average Performed:	3	1	3	3	1	3	3	3
Total Possible Core-ESs:	3	1	3	3	1	3	3	3
Used in RASSI:	3	1	3	3	**1**	**3**	**3**	**3**
Core-ES Triplets								
State-Average Performed:	3	1	3	3	1	3	3	3
Total Possible Core-ESs:	3	1	3	3	1	3	3	3
Used in RASSI:	3	1	3	3	**1**	**3**	**3**	**3**

Table S2: Number of state-average RASSCF roots and states used in subsequent RASSI calculations for RAS(S) O K-edge $[NpO_2]^{2+}$ XANES simulations. States in bold are those used when the Laporte selection rule was imposed. GS = Ground-State, Core-ES = Core-Excited State, VS = Valence State.

	AG	B1G	B2G	B3G	AU	B1U	B2U	B3U
GS Doublets								
State-Average Performed:					5	5	5	5
Used in RASSI:					**1**	**1**	**1**	**1**
VS Quartets								
State-Average Performed:					5	5	5	5
Used in RASSI:					**1**	**1**	**1**	**1**
Core-ES Doublets								
State-Average Performed:	28	24	24	24	24	28	24	24
Total Possible Core-ESs:	28	24	24	24	24	28	24	24
Used in RASSI:	**28**	**24**	**24**	**24**	24	28	24	24
Core-ES Quartets								
State-Average Performed:	9	12	12	12	12	9	12	12
Total Possible Core-ESs:	9	12	12	12	12	9	12	12
Used in RASSI:	**9**	**12**	**12**	**12**	12	9	12	12

Table S3: Number of state-average RASSCF roots and states used in subsequent RASSI calculations for RAS(S) U $M_{4/5}$-edge $[UO_2]^{2+}$ XANES simulations. GS = Ground-State, Core-ES = Core-Excited State.

	AG	AU	B1U	B2U	B3U
GS Singlet					
State-Average Performed:	5				
Used in RASSI:	1				
Core-ES Singlets					
State-Average Performed:		8	9	9	9
Total Possible Core-ESs:		8	9	9	9
Used in RASSI:		8	9	9	9
Core-ES Triplets					
State-Average Performed:		8	9	9	9
Total Possible Core-ESs:		8	9	9	9
Used in RASSI:		8	9	9	9

Table S4: Number of state-average RASSCF roots and states used in subsequent RASSI calculations for RAS(S) Np $M_{4/5}$-edge $[NpO_2]^{2+}$ XANES simulations. GS = Ground-State, Core-ES = Core-Excited State.

	AG	B1G	B2G	B3G	AU	B1U	B2U	B3U
GS Doublet								
State-Average Performed:					5	5	5	5
Used in RASSI:					1	1	1	1
Core-ES Doublets								
State-Average Performed:	62	61	61	61				
Total Possible Core-ESs:	62	61	61	61				
Used in RASSI:	62	61	61	61				
Used in RASSI (3654 eV Cutoff):	55	56	53	53				
Core-ES Quartets								
State-Average Performed:	24	27	27	27				
Total Possible Core-ESs:	24	27	27	27				
Used in RASSI:	24	27	27	27				
Used in RASSI (3654 eV Cutoff):	22	25	24	24				

Table S5: Number of state-average RASSCF roots and states used in subsequent RASSI calculations for RAS(SD) O K-edge $[UO_2]^{2+}$ XANES simulations. A max energy cut-off of 553 eV was utilized to inform choice of states used in RASSI. GS = Ground-State, Core-ES = Core-Excited State.

	AG	AU	B1U	B2U	B3U
GS Singlet					
State-Average Performed:	5				
Used in RASSI:	1				
Core-ES Singlets					
State-Average Performed:		145	155	155	155
Total Possible Core-ESs:		145	155	155	155
Used in RASSI:		62	63	68	68
Core-ES Triplets					
State-Average Performed:		217	221	221	221
Total Possible Core-ESs:		217	221	221	221
Used in RASSI:		93	90	95	95

Table S6: Number of state-average RASSCF roots and states used in subsequent RASSI calculations for RAS(SD) O K-edge $[NpO_2]^{2+}$ XANES simulations. A max energy cut-off of 547 eV was utilized to inform choice of states used in RASSI. GS = Ground-State, Core-ES = Core-Excited State.

	AG	B1G	B2G	B3G	AU	B1U	B2U	B3U
GS Doublet								
State-Average Performed:					5	5	5	5
Used in RASSI:					1	1	1	1
Core-ES Doublets								
State-Average Performed:	598	600	600	600				
Total Possible Core-ESs:	1192	1196	1196	1196				
Used in RASSI:	312	305	303	303				
Core-ES Quartets								
State-Average Performed:	600	600	600	600				
Total Possible Core-ESs:	843	874	874	874				
Used in RASSI:	234	239	233	233				

Table S7: Number of state-average RASSCF roots and states used in subsequent RASSI calculations for RAS(SD) U $M_{4/5}$-edge $[UO_2]^{2+}$ XANES simulations. A max energy cut-off of 3657 eV was utilized to inform choice of states used in RASSI. GS = Ground-State, Core-ES =

Core-Excited State.

	AG	AU	B1U	B2U	B3U
GS Singlet					
State-Average Performed:	5				
Used in RASSI:	1				
Core-ES Singlets					
State-Average Performed:		191	193	193	193
Total Possible Core-ESs:		191	193	193	193
Used in RASSI:		137	152	136	136
Core-ES Triplets					
State-Average Performed:		272	271	271	271
Total Possible Core-ESs:		272	271	271	271
Used in RASSI:		194	215	216	216

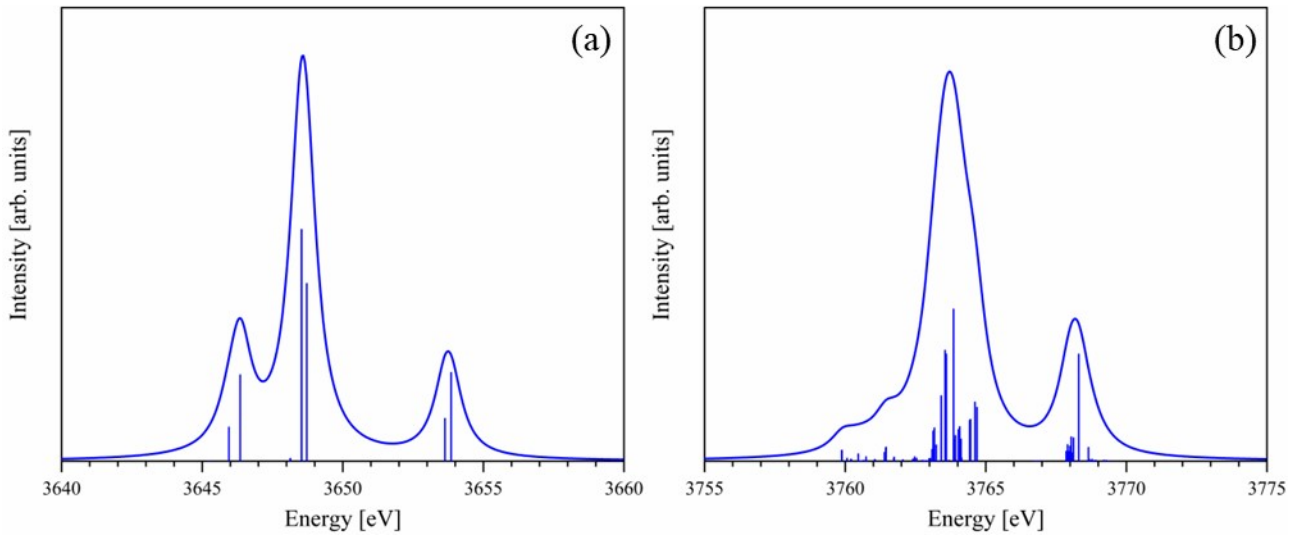

Figure S2: Spin-free RAS(S) spectra for (a) U M_4-edge of $[UO_2]^{2+}$ and (b) Np M_5-edge of $[NpO_2]^{2+}$ used to inform the energy cut-off values utilized to restrict RAS(SD) states utilized in RASSI calculations. Spin-free spectra were generated from state-interaction of GS and only irreps of singlet multiplicity for $[UO_2]^{2+}$ and doublets for $[NpO_2]^{2+}$. The number of states is recorded in tables S3 and S4.

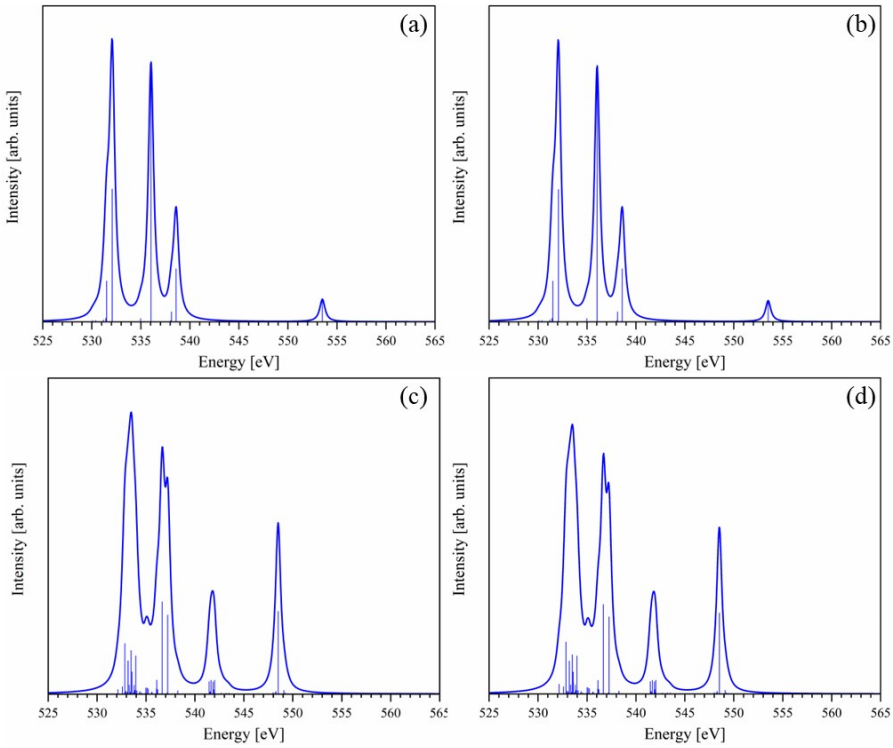

Figure S3: Oxygen K-edge XANES RAS(S) simulations for (a,b) $[UO_2]^{2+}$ and (c,d) $[NpO_2]^{2+}$ when (a,c) applying the Laporte selection rule and (b,d) without applying the rule, in order to inform the irreps supplied to RASSI calculations.

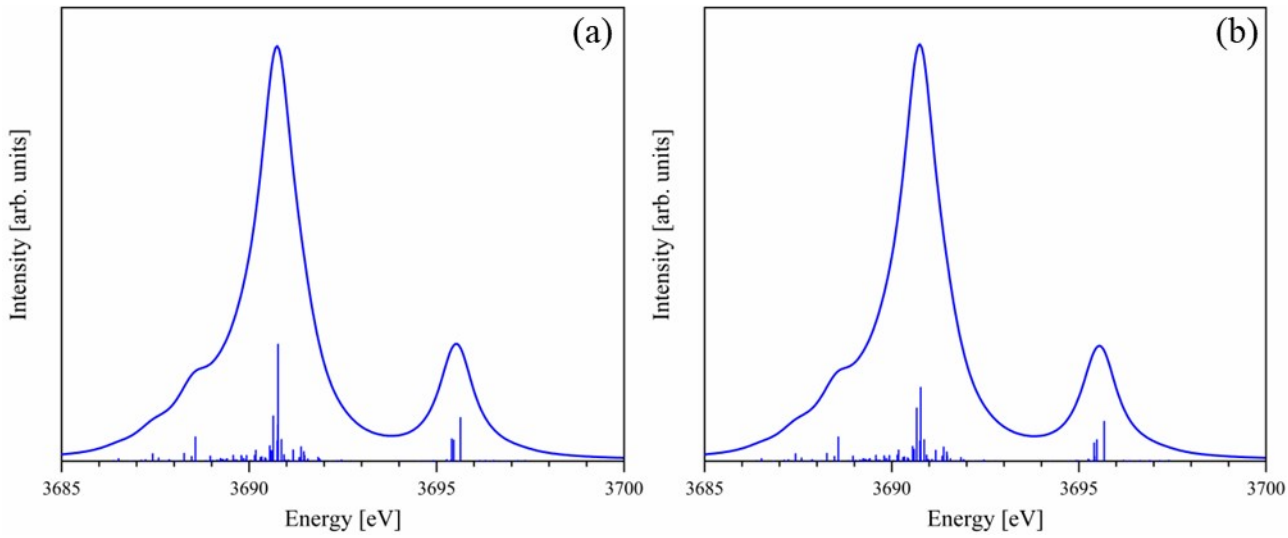

Figure S4: $[NpO_2]^{2+}$ Np M_5-edge XANES RAS(S) simulations when (a) including all possible core-excited stats in the RASSI calculation, and (b) when restricting states included in RASSI calculations informed by the 3773 eV cut-off for spin-free states. Cut-off was informed from figure S2(b).

3. Table of Energies for XANES Simulations:

Table S8: Peak energy positions in electron volts for RAS(SD) O K-Edge XANES simulations (unshifted), compared to experimental values for $[UO_2]^{2+}$ taken from experiment.[1] No reported O K-edge XANES experimental values are known for $[NpO_2]^{2+}$ so only RAS(SD) values are reported. Theoretical peak energies were measured as shown in figure S5 and S6, while state energies are taken from tables S20 and S21. Values reported in brackets are differences with respect to experimental peak positions. Detailed assignments of states and energies can be found in tables S20 and S21, and figures S9 and S10.

	$1s \rightarrow \delta/\phi$	$1s \rightarrow \pi_u^*$	$1s \rightarrow \sigma_u^*$	$1s \rightarrow \pi_g^*$	$1s \rightarrow \sigma_g^*$
$[UO_2]^{2+}$ O K-Edge					
Experiment:[1]	530.0	531.4	534.1	536.5	551.0
RAS(SD) Peak:	529.7 (-0.3)	531.7 (+0.3)	535.6 (+1.5)	537.1 (+0.6)	551.7 (+0.7)
RAS(SD) State:		State 24: 531.8 (0.4)	State 99: 535.6 (+1.5)	State 395: 537.2 (+0.7)	State 1377: 551.7 (+0.7)
RAS(SD) Peak – 0.3 eV:	529.4 (-0.6)	531.4 (0.0)	535.3 (+1.2)	536.8 (+0.3)	551.4 (+0.4)
$[NpO_2]^{2+}$ O K-Edge					
RAS(SD) Peak:	529.5	531.5	534.8	538.2	
RAS(SD) State:		State 45: 531.2	State 205: 534.8	State 1815: 538.2	

Table S9: Peak energy positions in electron volts for RAS(SD) $[NpO_2]^{2+}$ and $[UO_2]^{2+}$ An $M_{4/5}$-Edge XANES simulations, compared to experimental values taken from experiment.[2] Theoretical peak energies were measured as shown in figure S7 and S8, while state energies are taken from tables S22 and S24. Values reported in brackets are differences with respect to experimental peak positions. Detailed assignments of states and energies can be found in tables S22 and S24, and figures S12 and S16.

	$3d \rightarrow \delta/\phi$	$3d \rightarrow \pi_u^*$	$3d \rightarrow \sigma_u^*$
$[UO_2]^{2+}$ U M_4-Edge			
Experiment:[2]	3726.7	3728.8	3732.9
RAS(SD) Peak:	3748.6 (+21.9)	3750.5 (+21.7)	3754.1 (+21.2) / 3755.3 (+22.4)
RAS(SD) State:	State 2224: 3748.5 (+21.8)	State 2259: 3750.5 (+21.7)	State 2695 / State 2894: 3754.2 (+21.3) / 3755.1 (+22.2)
RAS(SD) Peak – 21.9 eV:	3726.7 (0.0)	3728.6 (-0.2)	3732.2 (-0.7) / 3733.4 (+0.5)
$[NpO_2]^{2+}$ Np M_5-Edge			
Approx. Experiment:[2]	3668.7	3668.7	3673.8
RAS(SD) Peak:	3688.5 (+19.8)	3690.4 (+21.7)	3695.3 (+21.5)
RAS(SD) State:	State 95/96: 3688.4 (+19.7)	State 309/310: 3690.4 (+21.7)	State 4557/4558: 3696.0 (+22.2)
RAS(SD) Peak – 21.7 eV:	3666.8 (-1.9)	3668.7 (0.0)	3673.6 (-0.2)

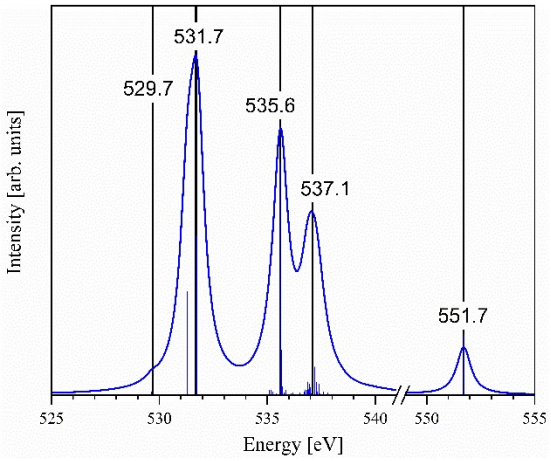

Figure S5: Peak energy measurements (eV) on the $[UO_2]^{2+}$ O K-edge XANES RAS(SD) simulated spectrum.

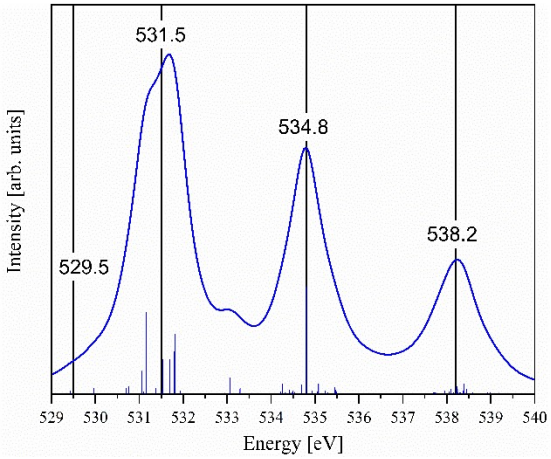

Figure S6: Peak energy measurements (eV) on the $[NpO_2]^{2+}$ O K-edge XANES RAS(SD) simulated spectrum.

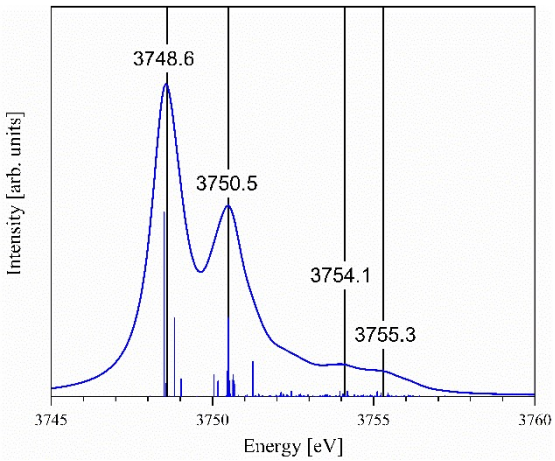

Figure S7: Peak energy measurements (eV) on the $[UO_2]^{2+}$ U M_4-edge XANES RAS(SD) simulated spectrum.

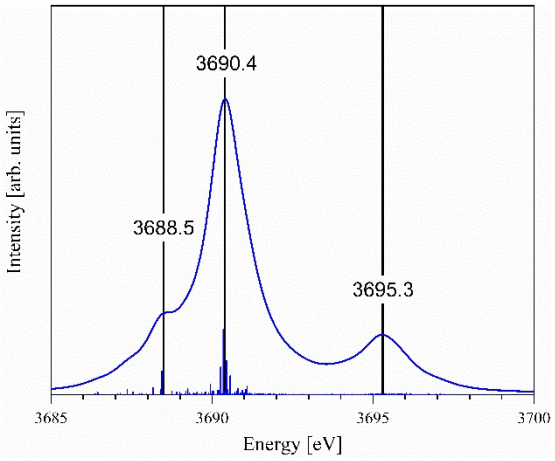

Figure S8: Peak energy measurements (eV) on the $[NpO_2]^{2+}$ Np M_5-edge XANES RAS(SD) simulated spectrum.

4. QTAIM Analysis:

Table S10: Changes in delocalisation $\Delta\delta(An,O)$ and localisation $\Delta\lambda(X)$ indexes between the ground- and core-excited states. States selected from $[AnO_2]^{2+}$ O K-edge RAS(SD), $[UO_2]^{2+}$ U M_4-edge and $[NpO_2]^{2+}$ Np M_5-edge RAS(SD) XANES simulations. Further QTAIM data can be examined in tables S12-15.

Core-Excitation	$\Delta\delta(An,O)$	$\Delta\lambda(An)$	$\Delta\lambda(O)$
$[UO_2]^{2+}$ O K-Edge			
$1s\rightarrow\pi_u^*$	-0.55	+0.71	+0.20
$1s\rightarrow\sigma_u^*$	-0.62	+0.83	+0.22
$1s\rightarrow\pi_g^*$	-0.68	+0.99	+0.21
$[NpO_2]^{2+}$ O K-Edge			
$1s\rightarrow\pi_u^*$	-0.47	+0.60	+0.17
$1s\rightarrow\sigma_u^*$	-0.58	+0.77	+0.21
$1s\rightarrow\pi_g^*$	-0.72	+0.96	+0.26
$[UO_2]^{2+}$ U M_4-Edge			
$3d\rightarrow\pi_u^*$	-0.19	+0.37	-0.01
$3d\rightarrow\sigma_u^*$	-0.37	+0.61	+0.07
$[NpO_2]^{2+}$ Np M_5-Edge			
$3d\rightarrow\pi_u^*$	-0.14	+0.38	-0.08
$3d\rightarrow\sigma_u^*$	-0.42	+0.54	+0.16

Table S11: Delocalisation $\delta(An,O)$ and localisation $\lambda(X)$ indexes for the ground- and core-excited states. The electron density at the bond critical point ρ_{BCP} is also reported in atomic units. States selected from $[AnO_2]^{2+}$ O K-edge RAS(SD), $[UO_2]^{2+}$ U M_4-edge and $[NpO_2]^{2+}$ Np M_5-edge RAS(SD) XANES simulations. Further QTAIM data can be examined in tables S12-15.

Core-Excitation	ρ_{BCP}	$\delta(An,O)$	$\lambda(An)$	$\lambda(O)$
$[UO_2]^{2+}$ O K-Edge				
GS	0.33	1.85	86.85	7.70
$1s \rightarrow \pi_u^*$	0.31	1.30	87.56	7.90
$1s \rightarrow \sigma_u^*$	0.32	1.23	87.68	7.91
$1s \rightarrow \pi_g^*$	0.29	1.17	87.83	7.91
$[NpO_2]^{2+}$ O K-Edge				
GS	0.30	1.73	87.95	7.77
$1s \rightarrow \pi_u^*$	0.28	1.26	88.55	7.94
$1s \rightarrow \sigma_u^*$	0.29	1.14	88.72	7.98
$1s \rightarrow \pi_g^*$	0.27	1.00	88.90	8.03
$[UO_2]^{2+}$ U M_4-Edge				
GS	0.33	1.85	86.67	7.78
$3d \rightarrow \pi_u^*$	0.32	1.65	87.05	7.77
$3d \rightarrow \sigma_u^*$	0.32	1.48	87.28	7.85
$[NpO_2]^{2+}$ Np M_5-Edge				
GS	0.34	1.86	87.83	7.69
$3d \rightarrow \pi_u^*$	0.34	1.72	88.21	7.61
$3d \rightarrow \sigma_u^*$	0.33	1.44	88.37	7.85

Table S12: QTAIM data for ground-state (GS) and a select number of key core-excited states from the $[UO_2]^{2+}$ O K-edge RAS(SD) XANES simulation. The electron-density at the bond critical point ρ_{BCP} in atomic units, delocalisation $\delta(U,O)$, and localisation indexes $\lambda(X)$ are reported. Changes in QTAIM metrics with respect to the GS are also reported (Δ).

	GS	$1s\rightarrow\pi_u^*$ Transition 1.4 State 24	Δ	$1s\rightarrow\sigma_u^*$ Transition 2.5 State 99	Δ	$1s\rightarrow\pi_g^*$ Transition 3.8 State 395	Δ	$1s\rightarrow\sigma_u^*$ Transition 4 State 1377	Δ
ρ_{BCP} (a.u.)	0.33	0.31	-0.03	0.32	-0.02	0.29	-0.04	0.32	-0.01
$\delta(U,O)$	1.85	1.30	-0.55	1.23	-0.62	1.17	-0.68	1.46	-0.39
$\lambda(U)$	86.85	87.56	0.71	87.68	0.83	87.83	0.99	87.38	0.53
$\lambda(O1)$	7.70	7.90	0.20	7.91	0.22	7.91	0.21	7.79	0.09
$\lambda(O2)$	7.70	7.90	0.20	7.91	0.21	7.91	0.21	7.79	0.09

Table S13: QTAIM data for ground-state (GS) and a select number of key core-excited states from the $[UO_2]^{2+}$ U M_4-Edge RAS(SD) XANES simulation. The electron-density at the bond critical point ρ_{BCP} in atomic units, delocalisation $\delta(U,O)$, and localisation indexes $\lambda(X)$ are reported. Changes in QTAIM metrics with respect to the GS are also reported (Δ).

	GS	$3d\rightarrow\pi_u^*$ Transition 2.4 State 2259	Δ	$3d\rightarrow\sigma_u^*$ Transition 3.11 State 2695	Δ	$3d\rightarrow\sigma_u^*$ Transition 3.14 State 2894	Δ
ρ_{BCP} (a.u.)	0.33	0.32	-0.02	0.32	-0.02	0.32	-0.02
$\delta(U,O)$	1.85	1.65	-0.19	1.48	-0.37	1.48	-0.37
$\lambda(U)$	86.67	87.05	0.37	87.28	0.61	87.27	0.60
$\lambda(O1)$	7.78	7.77	-0.01	7.85	0.07	7.86	0.08
$\lambda(O2)$	7.78	7.77	-0.01	7.85	0.07	7.86	0.08

Table S14: QTAIM data for ground-state (GS) and a select number of key core-excited states from the $[NpO_2]^{2+}$ O K-Edge RAS(SD) XANES simulation. The electron-density at the bond critical point ρ_{BCP} in atomic units, delocalisation $\delta(Np,O)$, and localisation indexes $\lambda(X)$ are reported. Changes in QTAIM metrics with respect to the GS are also reported (Δ).

	GS	$1s\rightarrow\pi_u^*$ Transition 1.6 State 45	Δ	$1s\rightarrow\sigma_u^*$ Transition 2.3 State 205	Δ	$1s\rightarrow\pi_g^*$ Transition 3.4 State 1815	Δ
ρ_{BCP} (a.u.)	0.30	0.28	-0.03	0.29	-0.01	0.27	-0.03
$\delta(Np,O)$	1.73	1.26	-0.47	1.14	-0.58	1.00	-0.72
$\lambda(Np)$	87.95	88.55	+0.60	88.72	+0.77	88.90	+0.96
$\lambda(O1)$	7.77	7.94	+0.17	7.98	+0.21	8.03	+0.26
$\lambda(O2)$	7.77	7.94	+0.17	7.98	+0.21	8.03	+0.26

Table S15: QTAIM data for ground-state (GS) and a select number of key core-excited states from the $[NpO_2]^{2+}$ Np M_5-Edge RAS(SD) XANES simulation. The electron-density at the bond critical point ρ_{BCP} in atomic units, delocalisation $\delta(Np,O)$, and localisation indexes $\lambda(X)$ are reported. Changes in QTAIM metrics with respect to the GS are also reported (Δ).

	GS	$3d\rightarrow\pi_u^*$ Transition 1.8 State 309	Δ	$3d\rightarrow\sigma_u^*$ Transition 2.5 State 4557	Δ
ρ_{BCP} (a.u.)	0.34	0.34	0.00	0.33	-0.01
$\delta(Np,O)$	1.86	1.72	-0.14	1.44	-0.42
$\lambda(Np)$	87.83	88.21	+0.38	88.37	+0.54
$\lambda(O1)$	7.69	7.61	-0.08	7.85	+0.16
$\lambda(O2)$	7.69	7.61	-0.08	7.85	+0.16

5. AIM Orbital Composition Analysis:

5.1 $[UO_2]^{2+}$ System:

Table S16: AIM orbital compositions for O K-Edge $[UO_2]^{2+}$ RAS(SD) XANES core-states. Values in brackets show overall change in composition between the ground- and core-excited states ($GS\% \rightarrow ES\%$).

Core-State	Orbital	U	O
$1s \rightarrow \pi_u^*$	π_u	$25\% \rightarrow 15\%$	$75\% \rightarrow 85\%$
Transition 1.4: State 24		(-10%)	$(+10\%)$
	π_u^*	$74\% \rightarrow 85\%$	$26\% \rightarrow 15\%$
		$(+11\%)$	(-11%)
$1s \rightarrow \sigma_u^*$	σ_u	$53\% \rightarrow 46\%$	$47\% \rightarrow 54\%$
Transition 2.5: State 99		(-7%)	$(+7\%)$
	σ_u^*	$50\% \rightarrow 68\%$	$50\% \rightarrow 32\%$
		$(+18\%)$	(-18%)
$1s \rightarrow \pi_g^*$	π_g	$17\% \rightarrow 9\%$	$83\% \rightarrow 91\%$
Transition 3.8: State 395		(-8%)	$(+8\%)$
	π_g^*	$45\% \rightarrow 75\%$	$55\% \rightarrow 25\%$
		$(+30\%)$	(-30%)
$1s \rightarrow \sigma_g^*$	σ_g	$19\% \rightarrow 14\%$	$81\% \rightarrow 86\%$
Transition 4: State 1377		(-4%)	$(+4\%)$
	σ_g^*	$48\% \rightarrow 61\%$	$52\% \rightarrow 39\%$
		$(+13\%)$	(-13%)

Table S17: AIM orbital compositions for U M_4-Edge $[UO_2]^{2+}$ RAS(SD) XANES core-states. Values in brackets show overall change in composition between the ground- and core-excited states ($GS\% \rightarrow ES\%$).

Core-State	Orbital	U	O
$3d \rightarrow \pi_u^*$	π_u	$26\% \rightarrow 26\%$	$74\% \rightarrow 74\%$
Transition 2.4: State 2259		(0%)	(0%)
	π_u^*	$74\% \rightarrow 77\%$	$26\% \rightarrow 23\%$
		$(+3\%)$	(-3%)
$3d \rightarrow \sigma_u^*$	σ_u	$56\% \rightarrow 57\%$	$44\% \rightarrow 43\%$
Transition 3.11: State 2695		$(+1\%)$	(-1%)
	σ_u^*	$56\% \rightarrow 58\%$	$44\% \rightarrow 42\%$
		$(+2\%)$	(-2%)
$3d \rightarrow \sigma_u^*$	σ_u	$56\% \rightarrow 56\%$	$44\% \rightarrow 44\%$
Transition 3.14: State 2894		(0%)	(0%)
	σ_u^*	$56\% \rightarrow 59\%$	$44\% \rightarrow 41\%$
		$(+3\%)$	(-3%)

5.2 $[NpO_2]^{2+}$ System:

Table S18: AIM orbital compositions for O K-Edge $[NpO_2]^{2+}$ RAS(SD) XANES core-states. Values in brackets show overall change in composition between the ground- and core-excited states ($GS\% \rightarrow ES\%$).

Core-State	Orbital	Np	O
$1s \rightarrow \pi_u^*$	π_u	$28\% \rightarrow 15\%$	$72\% \rightarrow 83\%$
Transition 1.6: State 45/46		(-13%)	$(+13\%)$
	π_u^*	$71\% \rightarrow 84\%$	$29\% \rightarrow 16\%$
		$(+13\%)$	(-13%)
$1s \rightarrow \sigma_u^*$	σ_u	$55\% \rightarrow 54\%$	$45\% \rightarrow 46\%$
Transition 2.3: State 205		(-1%)	$(+1\%)$
	σ_u^*	$61\% \rightarrow 71\%$	$39\% \rightarrow 29\%$
		$(+10\%)$	(-10%)
$1s \rightarrow \pi_g^*$	π_g	$16\% \rightarrow 10\%$	$84\% \rightarrow 90\%$
Transition 3.4: State 1815/1816		(-6%)	$(+6\%)$
	π_g^*	$61\% \rightarrow 74\%$	$39\% \rightarrow 26\%$
		$(+13\%)$	(-13%)

Table S19: AIM orbital composition for Np M_5-Edge $[NpO_2]^{2+}$ RAS(SD) XANES core-states. Values in brackets show overall change in composition between the ground- and core-excited states ($GS\% \rightarrow ES\%$).

Core-State	Orbital	Np	O
$3d \rightarrow \pi_u^*$	π_u	$27\% \rightarrow 28\%$	$73\% \rightarrow 72\%$
Transition 1.8: State 309		$(+1\%)$	(-1%)
	π_u^*	$73\% \rightarrow 75\%$	$27\% \rightarrow 25\%$
		$(+2\%)$	(-2%)
$3d \rightarrow \sigma_u^*$	σ_u	$62\% \rightarrow 60\%$	$38\% \rightarrow 40\%$

Transition 2.5: State 4557/4558		(− 2%)	(+ 2%)
	σ_u^*	55% →55%	45% →45%
		(0%)	(0%)

6. Additional Theoretical Spectra & Assignments at the RAS(SD) Level of Theory:

6.1 $[UO_2]^{2+}$ and $[NpO_2]^{2+}$ O K-edge XANES assignments:

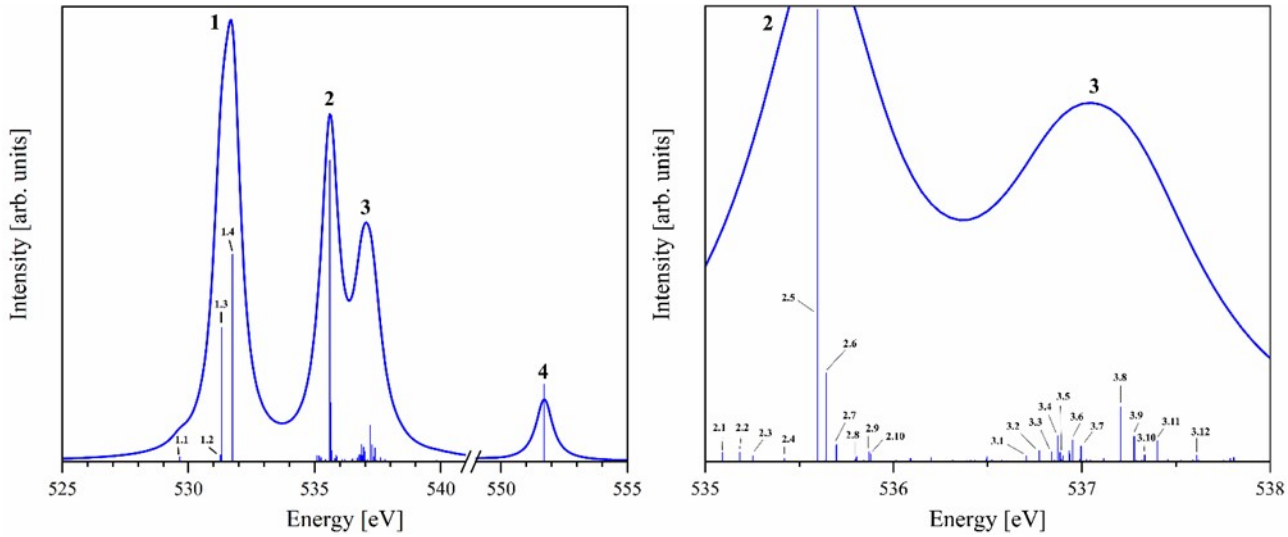

Figure S9: Theoretical oxygen K-edge $[UO_2]^{2+}$ RAS(SD) XANES spectrum annotated with peak and stick transition labels. The 525-555 eV (left) and a 535-538 eV (right) region is shown. Assignments of labelled transitions can be found in table S20.

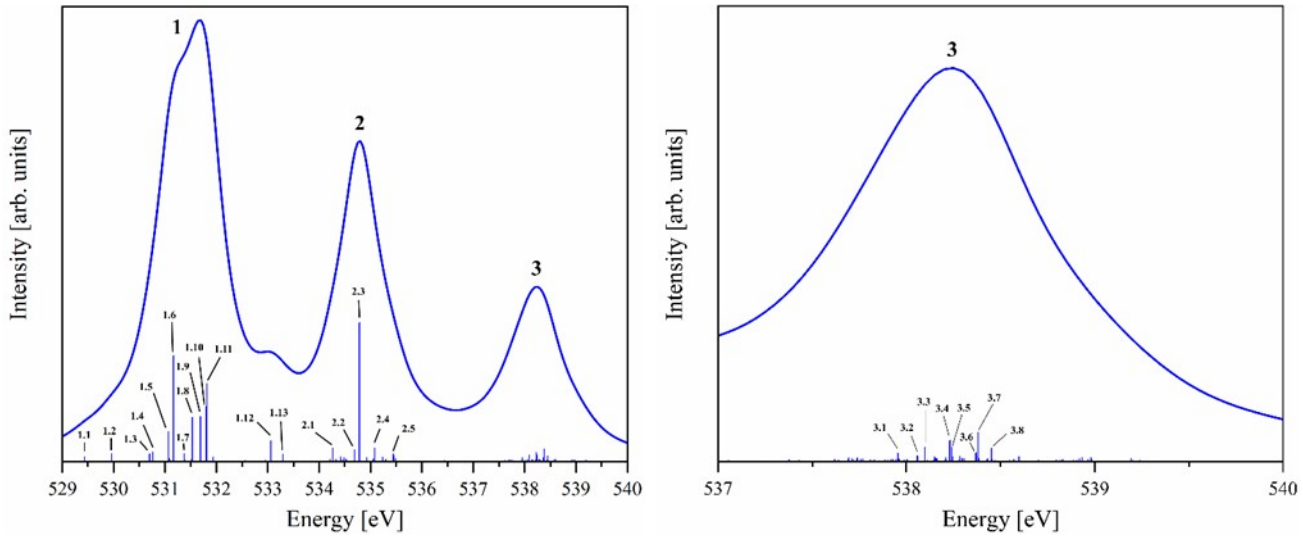

Figure S10: Theoretical oxygen K-edge $[NpO_2]^{2+}$ RAS(SD) XANES spectrum annotated with peak and stick transition labels. The 529 – 540 eV (left) and 537 – 540 eV (right) regions are shown. Assignments of labelled transitions can be found in table S21.

6.2 $[UO_2]^{2+}$ O K-Edge RAS(SD) XANES:

Peak 1 in figure S9, contains two high intensity transitions labelled 1.3 and 1.4, which correspond to clear core-excitations into the π^*_u orbitals. A low intensity transition, 1.1, assigned to core-excitation into the non-bonding 5f orbitals is also found. This would indicate that the non-bonding 5f orbitals fall at lower orbital energy than the π^*_u. Peak 2 is assigned to a core-excitation into the σ^*_u, the highest intensity transition labelled 2.5 has a σ^*_u natural occupation of 0.68, with the remaining natural occupation residing in the non-bonding 5f orbitals. States labelled from 2.1 to 2.10, which are distributed either side of the 2.5 transition, do not contain significant σ^*_u occupation, rather these states correspond to core-excitations primarily into the 5f non-bonding orbitals, and to a lower degree the π^*_u orbitals. It is the two lowest energy orbitals which are utilized first with partial electron occupation to minimize the state energy, with the lower energy non-bonding 5f orbitals being utilized to the greater degree, followed by the π^*_u orbitals. This trend continues as states become more multiconfigurational under peak 3. Transitions labelled 3.1 – 3.12 all contain varying degrees of π^*_g natural orbital occupation. The highest π^*_g occupation is for transitions 3.8 and 3.10, with 3.8 being the most intense state out of the set of 12 transitions. Peak 3 is assigned to core-excitation into the π^*_g orbitals, as transitions under this peak contains π^*_g occupation at a greater level above that of all other states. Peak 4 contains a core-excitation responsible for generating the peak, assigned to core-excitation into the σ^*_g orbital. Overall, the same core-excitation assignments for peaks 1-4 can be made here at the RAS(SD) level as compared with RAS(S). Detailed assignments are given in table S20.

Table S20: Assignments for $[UO_2]^{2+}$ oxygen K-edge XANES RAS(SD) simulation. Table reports the natural populations of the spin-orbit natural orbitals for key core-states. Transitions correspond to assignments made in figure S9. States corresponds to the spin-orbit coupled state numbers assigned by the OpenMolcas RASSI calculation. Energy corresponds to the state energy in electron-volts.

Transition	State	Energy	1s(g)	1s(u)	σu*	πu*	πg*	σg*	φu	δu
	GS	0	2.00	2.00	0.05	0.04/0.04	0.02/0.02	0.01	0.00/0.00	0.00/0.00
1.1	8/9	529.65	1.24	1.76	0.08	0.06/0.06	0.05/0.05	0.00	0.00/0.00	0.48/0.48
1.2	19	531.28	1.27	1.73	0.09	0.50/0.50	0.09/0.09	0.00	0.00/0.00	0.01/0.01
1.3	20/21	531.31	1.27	1.73	0.09	0.59/0.41	0.09/0.07	0.00	0.00/0.00	0.01/0.01
1.4	24/25	531.76	1.27	1.73	0.08	0.59/0.40	0.08/0.08	0.00	0.00/0.00	0.02/0.02
2.1	60/61	535.09	1.36	1.64	0.50	0.10/0.09	0.04/0.04	0.01	0.10/0.09	0.36/0.35
2.2	67	535.18	1.46	1.54	0.03	0.10/0.10	0.01/0.01	0.00	0.23/0.23	0.63/0.63
2.3	71	535.25	1.42	1.58	0.01	0.06/0.06	0.00/0.00	0.00	0.30/0.30	0.63/0.63
2.4	80	535.42	1.43	1.57	0.01	0.11/0.11	0.00/0.00	0.00	0.27/0.27	0.62/0.61
2.5	99	535.60	1.32	1.68	0.68	0.08/0.08	0.04/0.04	0.01	0.09/0.09	0.23/0.23
2.6	109	535.64	1.44	1.56	0.13	0.09/0.09	0.02/0.02	0.00	0.23/0.22	0.60/0.52
2.7	118	535.70	1.44	1.56	0.04	0.13/0.12	0.01/0.01	0.00	0.29/0.29	0.57/0.53
2.8	129	535.80	1.44	1.56	0.01	0.14/0.14	0.01/0.01	0.00	0.34/0.33	0.53/0.51
2.9	145	535.87	1.46	1.54	0.02	0.06/0.06	0.01/0.01	0.00	0.38/0.38	0.60/0.46
2.10	148	535.88	1.47	1.53	0.02	0.06/0.06	0.01/0.01	0.00	0.39/0.39	0.59/0.45
3.1	296	536.71	1.45	1.55	0.03	0.39/0.38	0.02/0.02	0.00	0.30/0.30	0.28/0.26
3.2	309/310	536.77	1.47	1.53	0.03	0.47/0.67	0.05/0.02	0.00	0.27/0.25	0.27/0.26
3.3	317/318	536.84	1.47	1.53	0.04	0.44/0.31	0.06/0.05	0.00	0.37/0.24	0.26/0.19
3.4	324/325	536.87	1.49	1.51	0.04	0.33/0.31	0.10/0.06	0.00	0.36/0.27	0.25/0.22
3.5	327	536.88	1.46	1.54	0.03	0.42/0.41	0.02/0.02	0.00	0.26/0.26	0.29/0.29
3.6	342/343	536.95	1.49	1.51	0.04	0.44/0.36	0.10/0.02	0.00	0.22/0.21	0.30/0.27
3.7	352/353	537.00	1.48	1.52	0.04	0.40/0.34	0.08/0.07	0.00	0.25/0.16	0.31/0.29
3.8	395/396	537.21	1.52	1.48	0.05	0.29/0.25	0.20/0.06	0.00	0.33/0.32	0.20/0.17

3.9	406/407	537.28	1.49	1.51	0.03	0.32/0.30	0.09/0.02	0.00	0.44/0.42	0.19/0.14
3.10	419/420	537.33	1.48	1.52	0.05	0.22/0.26	0.21/0.05	0.00	0.28/0.33	0.24/0.23
3.11	433/434	537.40	1.49	1.51	0.02	0.39/0.36	0.10/0.02	0.00	0.29/0.27	0.28/0.21
3.12	480/481	537.61	1.46	1.54	0.05	0.37/0.36	0.05/0.04	0.00	0.25/0.23	0.32/0.29
4	1377	551.71	1.74	1.26	0.13	0.11/0.11	0.04/0.04	0.97	0.00/0.00	0.00/0.00

6.3 $[NpO_2]^{2+}$ O K-Edge RAS(SD) XANES:

The RAS(SD) simulated O k-edge spectrum of $[NpO_2]^{2+}$, figure S10, contains the correct three-peak structure in the 525-545 eV energy range. To make simulation tractable, a 545 eV energy cut-off was utilized when performing the state-interaction (RASSI) calculation. Therefore, peak 4 captured at the RAS(S) level, is neglected here as it does not fall within the energy threshold. The overall assignments for peaks 1-3, are the same as those made at the RAS(S) level of theory. Peak 1 is assigned to a core-excitation into π^*_u, peak 2 into σ^*_u and peak 3 into π^*_g. Peak 1 contains a higher density of states compared to RAS(S), with transitions labelled 1.5 – 1.13 containing significant π^*_u occupation. States 1.1 – 1.4 which contribute to a small intensity shoulder on the first peak are assigned to core-excitations into the non-bonding 5f orbitals. Peak 2 contains a number of transitions, 2.1 – 2.5, which contain significant σ^*_u occupancy. State 2.3 is the most intense of these and corresponds to the state with the highest σ^*_u occupancy. For these states, there is also significant additional occupancy of the non-bonding 5f orbitals and to a lesser degree π^*_u occupancy. Peak 3 contains states presenting higher degrees of multiconfigurational character. The high density of states is labelled 3.1 – 3.12, of which 3.4, 3.5, 3.7 and 3.8, contain higher than the background level occupation of the π^*_g orbitals. States continue an emerging trend for these RAS(SD) simulations, shared for $[UO_2]^{2+}$ and $[NpO_2]^{2+}$ O k-edge, as higher energy core-states tend to utilize occupation of lower energy orbitals to optimize states. The exception to this being for peak 4 which has near single electron occupancy of the σ^*_g orbital. Detailed assignments given in table S21.

Table S21: Assignments for $[NpO_2]^{2+}$ oxygen K-edge XANES RAS(SD) simulation. Table reports the natural populations of the spin-orbit natural orbitals for key core-states. Transitions correspond to assignments made in figure S10. States corresponds to the spin-orbit coupled state numbers assigned by the OpenMolcas RASSI calculation. Energy corresponds to the state energy in electron-volts.

Transition	State	Energy	1s(g)	1s(u)	σu*	πu*	πg*	σg*	φu	δu
	GS	0	2.00	2.00	0.05	0.08/0.08	0.02/0.02	0.01	0.45/0.44	0.06/0.06
1.1	12/11	529.44	1.26	1.74	0.08	0.08/0.08	0.04/0.04	0.01	0.48/0.47	0.50/0.50
1.2	17/18	529.96	1.26	1.74	0.08	0.13/0.13	0.05/0.05	0.01	0.34/0.34	0.58/0.58
1.3	27/28	530.70	1.26	1.74	0.08	0.11/0.11	0.04/0.04	0.01	0.32/0.32	0.62/0.62
1.4	29/30	530.77	1.26	1.74	0.08	0.19/0.19	0.05/0.05	0.01	0.40/0.40	0.47/0.46
1.5	39/40	531.07	1.27	1.73	0.09	0.41/0.41	0.06/0.06	0.02	0.36/0.36	0.26/0.26
1.6	46/45	531.16	1.26	1.74	0.08	0.31/0.31	0.05/0.05	0.02	0.25/0.25	0.49/0.49
1.7	48/47	531.38	1.28	1.72	0.10	0.51/0.51	0.07/0.07	0.02	0.07/0.07	0.44/0.43
1.8	55/56	531.54	1.27	1.73	0.10	0.46/0.46	0.06/0.06	0.02	0.42/0.42	0.15/0.14
1.9	62/61	531.69	1.26	1.74	0.08	0.22/0.22	0.05/0.05	0.01	0.43/0.43	0.41/0.41
1.10	63/64	531.80	1.27	1.73	0.08	0.50/0.50	0.06/0.06	0.01	0.45/0.45	0.09/0.09
1.11	69/70	531.82	1.27	1.73	0.07	0.43/0.43	0.06/0.06	0.01	0.45/0.45	0.18/0.17
1.12	116/115	533.06	1.28	1.72	0.09	0.41/0.41	0.06/0.06	0.02	0.38/0.37	0.25/0.25
1.13	121/122	533.29	1.28	1.72	0.22	0.46/0.46	0.06/0.06	0.02	0.08/0.08	0.43/0.42
2.1	156/155	534.27	1.30	1.70	0.60	0.42/0.42	0.06/0.06	0.04	0.24/0.24	0.14/0.14
2.2	195/196	534.70	1.45	1.55	0.20	0.37/0.37	0.02/0.02	0.01	0.41/0.41	0.55/0.55
2.3	206/205	534.79	1.33	1.67	0.72	0.20/0.20	0.03/0.03	0.03	0.45/0.45	0.21/0.21
2.4	248/247	535.08	1.45	1.55	0.17	0.39/0.35	0.01/0.01	0.01	0.47/0.46	0.53/0.53
2.5	332/331	535.44	1.41	1.59	0.33	0.32/0.30	0.02/0.02	0.02	0.45/0.44	0.44/0.44
3.1	1644/1643	537.96	1.45	1.55	0.29	0.42/0.42	0.05/0.04	0.01	0.43/0.43	0.45/0.40
3.2	1707/1708	538.06	1.47	1.53	0.26	0.41/0.41	0.04/0.04	0.01	0.38/0.38	0.52/0.52

3.3	1736/1735	538.10	1.46	1.54	0.19	0.38/0.38	0.07/0.07	0.01	0.45/0.44	0.49/0.49
3.4	1816/1815	538.23	1.50	1.50	0.24	0.40/0.39	0.12/0.12	0.01	0.43/0.41	0.40/0.39
3.5	1826/1825	538.24	1.49	1.51	0.23	0.40/0.39	0.11/0.10	0.01	0.42/0.39	0.44/0.43
3.6	1899/1900	538.37	1.47	1.53	0.28	0.37/0.37	0.07/0.07	0.01	0.45/0.44	0.45/0.45
3.7	1906/1905	538.38	1.52	1.48	0.19	0.40/0.39	0.21/0.14	0.01	0.36/0.35	0.40/0.39
3.8	1942/1941	538.45	1.51	1.49	0.19	0.38/0.38	0.16/0.15	0.01	0.42/0.42	0.39/0.38

6.4 RAS(SD) Assignments for Simulated Uranium $M_{4/5}$-edge XANES:

Figure S11 shows the spin-orbit splitting between the M_5- and M_4-edges for $[UO_2]^{2+}$ and $[NpO_2]^{2+}$, with the splitting for $[UO_2]^{2+}$ of 172 eV being consistent with previously reported values.[3]

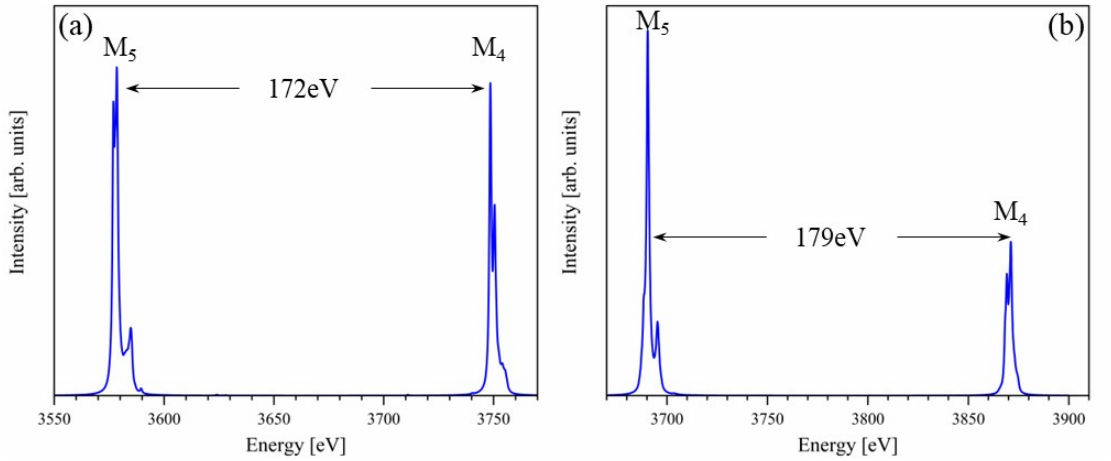

Figure S11: Theoretical (a) $[UO_2]^{2+}$ and (b) $[NpO_2]^{2+}$ U/Np $M_{4/5}$-edge XANES RAS(SD) spectrum showing the spin-orbit coupling splitting between the M_5- and M_4-edges.

6.5 $[UO_2]^{2+}$ U $M_{4/5}$-Edge RAS(SD) XANES:

Figure S12 shows the U M_4-edge simulated XANES spectrum at the RAS(SD) level of theory consisting of three peaks 1-3. The same overall peak assignments made for the RAS(S) spectrum are utilized to inform and aid in the assignments made here, as states present more multiconfigurational character, making assignments more difficult. However, we find that the assignments made here are in agreement with the RAS(S) simulations, with peaks 1, 2 and 3 corresponding to core-excitations into the non-bonding 5f, π^*_u, and σ^*_u orbitals respectively, and further agree with those made by Vitova *et al.*[2] Peak 1 contains transitions labelled 1.1 – 1.4 which are assigned to core-excitations into the non-bonding 5f orbitals. Peak 2 contains transitions labelled 2.1 – 2.8, which show clear occupation of the π^*_u orbitals, alongside partial occupation of the non-boding 5f orbitals. Peak 3 contains a large density of states, transitions labelled 3.1 – 3.8 consist of core-states with substantial partial occupations of both the non-bonding 5f orbitals and π^*_u. While transitions 3.9 – 3.16 (except 3.15), show low level occupation of the σ^*_u, these are found to be higher than the background level occupancy, which combined with RAS(S) findings, allows for the conclusion that these states represent core-excitations into the σ^*_u. Transitions 3.9 and 3.16 present core-states with the greatest σ^*_u occupancy at 0.14 and 0.17 respectively. Detailed assignments given in table S22.

Figures S13-14 show the U M_5-edge RAS(SD) simulated XANES spectrum consisting of two main peaks. Peak 1 contains a number of transitions labelled 1.1 – 1.10 show non-bonding 5f and π^*_u orbital occupancy. Natural populations therefore indicate that peak 1 contains core-states with an admixture of both non-bonding 5f and π^*_u occupancy. Transitions labelled 2.1 – 2.6, also show the same occupancy pattern. Transitions 2.7 – 2.17 all show clear σ^*_u occupancy above the background

level, with states 2.10, 2.12 and 2.17 all having the highest degrees of σ_u^* occupation at 0.34, 0.35 and 0.41 respectively. Detailed assignments given in table S23.

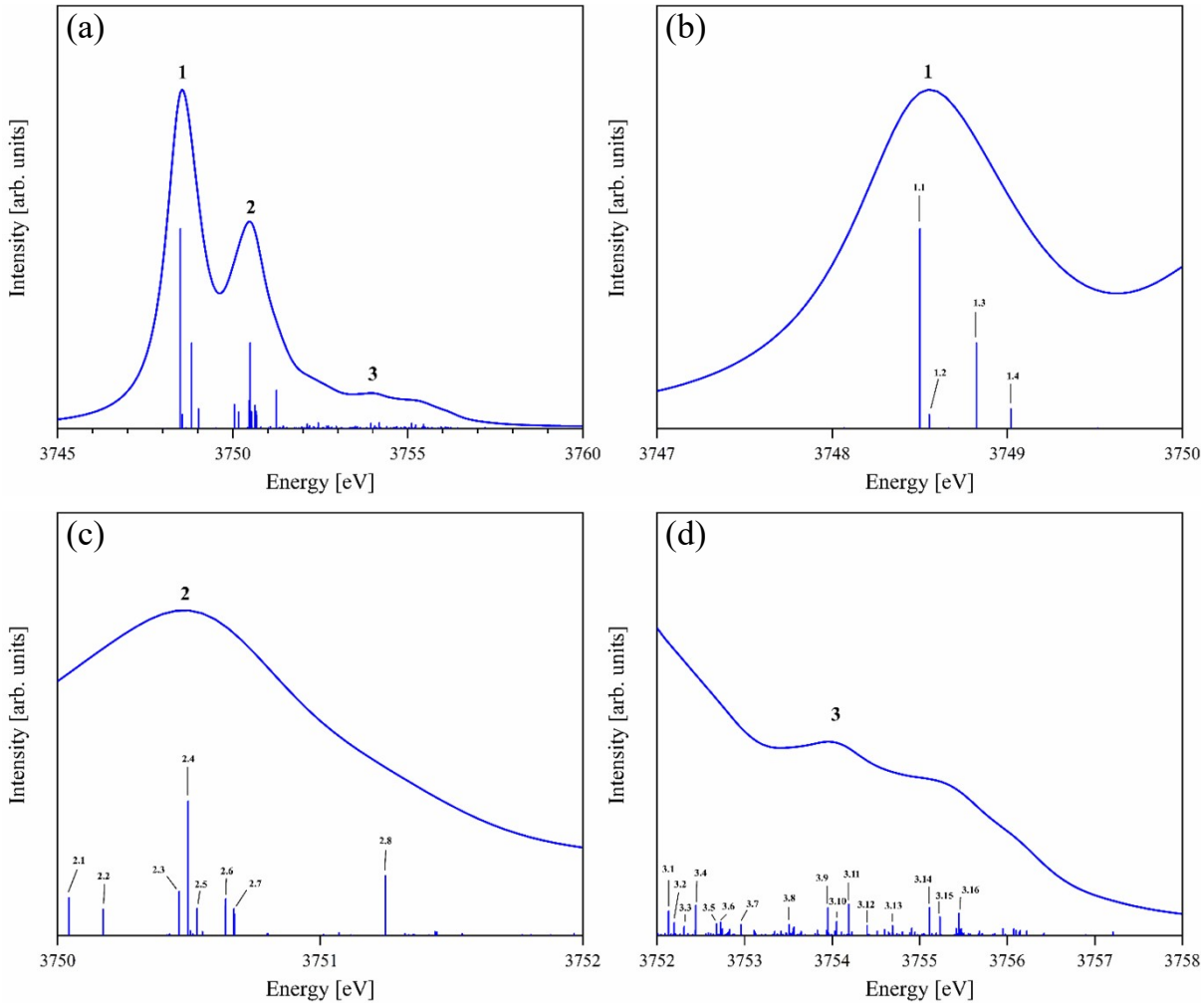

Figure S12: (a) The theoretical RAS(SD) $[UO_2]^{2+}$ U M_4-edge XANES spectrum and (b-d) peak regions. Spectra are annotated with peak and stick transition labels. Assignments of labelled transitions can be found in table S22.

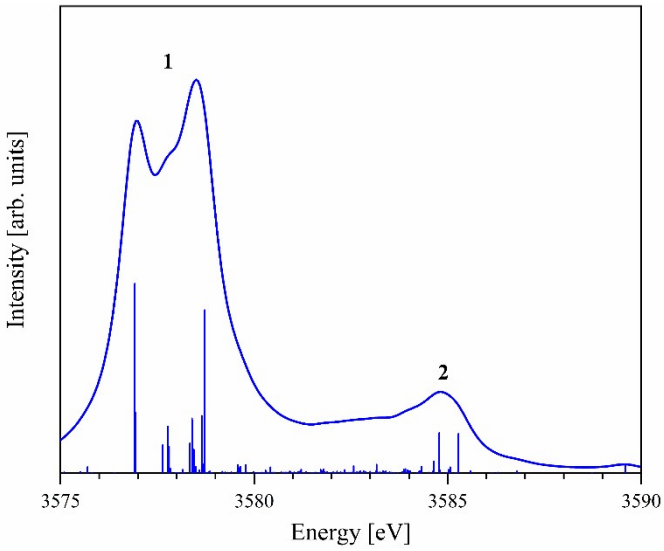

Figure S13: The theoretical RAS(SD) $[UO_2]^{2+}$ U M_5-edge XANES spectrum annotated with peak labels.

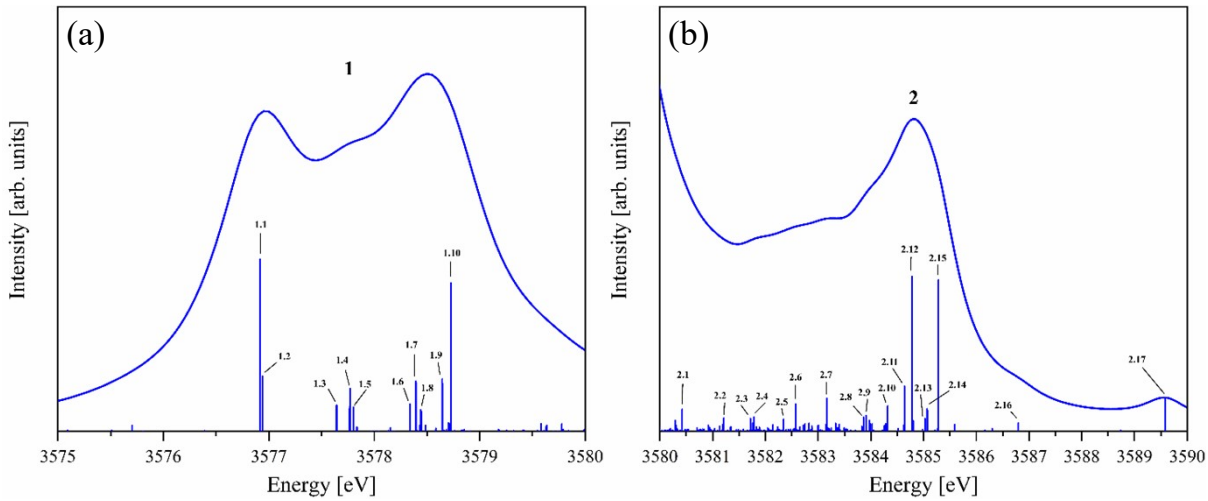

Figure S14: The theoretical RAS(SD) $[UO_2]^{2+}$ U M_5-edge XANES spectrum split into the two peak regions (a) 3575-3580 eV and (b) 3580 – 3590 eV. Spectra are annotated with peak and stick transition labels. Assignments of labelled transitions can be found in table S23.

Table S22: Assignments for M_4-edge XANES states for $[UO_2]^{2+}$ at the RAS(SD) level of theory. Table reports the natural populations of the spin-orbit natural orbitals for key core-states. Transitions correspond to assignments made in figure S12. States corresponds to the spin-orbit coupled state numbers assigned by the OpenMolcas RASSI calculation. Energy corresponds to the state energy in electron-volts.

Transition	State	Energy	3d	3d	3d	3d	3d	σu*	πu*	φu	δu
	GS	0	2.00	2.00	2.00	2.00	2.00	0.04	0.04/0.04	0.00/0.00	0.01/0.01
1.1	2224/2225	3748.50	1.87	1.73	1.73	1.86	1.81	0.01	0.02/0.02	0.38/0.34	0.17/0.11
1.2	2226/2227	3748.55	1.64	1.96	1.96	1.73	1.71	0.01	0.02/0.01	0.61/0.20	0.13/0.06
1.3	2232	3748.82	1.99	1.61	1.61	1.90	1.90	0.01	0.02/0.02	0.01/0.01	0.49/0.49
1.4	2235/2236	3749.02	1.98	1.62	1.62	1.89	1.89	0.01	0.03/0.01	0.02/0.02	0.49/0.48
2.1	2242/2243	3750.04	1.66	1.92	1.92	1.76	1.73	0.06	0.72/0.31	0.05/0.04	0.18/0.15
2.2	2247/2248	3750.17	1.69	1.89	1.87	1.82	1.72	0.05	0.53/0.48	0.09/0.08	0.20/0.19
2.3	2257	3750.46	1.69	1.91	1.91	1.76	1.73	0.01	0.16/0.15	0.33/0.33	0.42/0.41
2.4	2259	3750.50	1.65	1.95	1.95	1.74	1.71	0.02	0.37/0.28	0.16/0.14	0.28/0.24

2.5	2263/2264	3750.53	1.92	1.73	1.68	1.92	1.76	0.02	0.26/0.22	0.25/0.23	0.35/0.33
2.6	2270	3750.64	1.88	1.73	1.72	1.88	1.80	0.02	0.26/0.13	0.26/0.25	0.45/0.36
2.7	2271	3750.67	1.63	1.96	1.96	1.74	1.70	0.02	0.27/0.17	0.24/0.23	0.40/0.38
2.8	2310	3751.25	1.86	1.74	1.74	1.83	1.82	0.02	0.35/0.34	0.14/0.14	0.27/0.23
3.1	2376	3752.13	1.71	1.89	1.89	1.78	1.73	0.02	0.14/0.11	0.34/0.32	0.55/0.49
3.2	2382	3752.20	1.82	1.78	1.78	1.81	1.81	0.01	0.06/0.06	0.25/0.25	0.67/0.67
3.3	2393	3752.31	1.83	1.78	1.77	1.83	1.80	0.02	0.26/0.23	0.44/0.39	0.39/0.26
3.4	2408	3752.44	1.76	1.84	1.82	1.82	1.76	0.01	0.13/0.09	0.39/0.39	0.48/0.47
3.5	2440	3752.68	1.91	1.70	1.69	1.87	1.83	0.02	0.39/0.30	0.41/0.41	0.24/0.22
3.6	2451	3752.73	1.87	1.75	1.73	1.87	1.79	0.01	0.20/0.13	0.46/0.37	0.42/0.40
3.7	2497	3752.96	1.89	1.72	1.71	1.85	1.83	0.01	0.13/0.12	0.41/0.41	0.46/0.45
3.8	2590	3753.51	1.73	1.87	1.87	1.79	1.75	0.02	0.22/0.20	0.42/0.38	0.46/0.29
3.9	2659	3753.95	1.70	1.90	1.90	1.76	1.74	0.14	0.26/0.25	0.36/0.36	0.29/0.25
3.10	2674	3754.05	1.71	1.89	1.89	1.77	1.75	0.11	0.26/0.30	0.40/0.42	0.20/0.24
3.11	2695	3754.19	1.69	1.91	1.91	1.74	1.74	0.10	0.37/0.37	0.34/0.34	0.22/0.21
3.12	2737	3754.40	1.85	1.75	1.75	1.82	1.82	0.07	0.43/0.43	0.17/0.16	0.35/0.35
3.13	2807	3754.69	1.72	1.88	1.88	1.76	1.76	0.07	0.40/0.39	0.25/0.25	0.34/0.27
3.14	2894	3755.11	1.75	1.85	1.85	1.77	1.77	0.08	0.45/0.44	0.22/0.22	0.29/0.26
3.15	2916	3755.23	1.70	1.90	1.90	1.75	1.75	0.03	0.52/0.51	0.14/0.14	0.33/0.31
3.16	2949	3755.45	1.72	1.88	1.87	1.78	1.75	0.17	0.42/0.40	0.18/0.17	0.29/0.27

Table S23: Assignments for M_5-edge XANES for $[UO_2]^{2+}$ at the RAS(SD) level of theory. Table reports the natural populations of the spin-orbit natural orbitals for key core-states. Transitions correspond to assignments made in figures S13 and S14. States corresponds to the spin-orbit coupled state numbers assigned by the OpenMolcas RASSI calculation. Energy corresponds to the state energy in electron-volts.

Transition	State	Energy	3d	3d	3d	3d	3d	σu*	πu*	φu	δu
	GS	0	2.00	2.00	2.00	2.00	2.00	0.04	0.04/0.04	0.00/0.00	0.01/0.01
1.1	47/48	3576.92	1.87	1.76	1.75	1.83	1.80	0.01	0.16/0.04	0.27/0.26	0.17/0.16
1.2	49	3576.94	1.97	1.54	1.53	1.98	1.98	0.01	0.04/0.04	0.03/0.03	0.45/0.45
1.3	62/63	3577.64	1.55	1.98	1.96	1.98	1.53	0.02	0.73/0.14	0.05/0.05	0.10/0.10
1.4	73	3577.77	1.45	1.98	1.98	1.82	1.78	0.03	0.43/0.41	0.06/0.06	0.13/0.13
1.5	75/76	3577.8	1.69	1.96	1.91	1.76	1.67	0.02	0.30/0.19	0.22/0.20	0.36/0.35
1.6	114/115	3578.34	1.67	1.90	1.85	1.92	1.66	0.01	0.19/0.09	0.30/0.30	0.47/0.46
1.7	120	3578.39	1.81	1.72	1.65	1.92	1.90	0.01	0.27/0.13	0.24/0.23	0.43/0.39
1.8	126	3578.44	1.89	1.83	1.65	1.91	1.72	0.01	0.18/0.09	0.39/0.31	0.43/0.43
1.9	140	3578.65	1.99	1.58	1.56	1.94	1.94	0.01	0.40/0.38	0.08/0.08	0.19/0.19
1.10	149	3578.73	1.95	1.90	1.89	1.63	1.63	0.02	0.38/0.38	0.09/0.08	0.20/0.18
2.1	403	3580.42	1.78	1.83	1.76	1.82	1.81	0.00	0.13/0.12	0.34/0.34	0.54/0.51
2.2	600	3581.21	1.68	1.90	1.90	1.76	1.76	0.02	0.24/0.23	0.45/0.45	0.33/0.26
2.3	719	3581.72	1.67	1.87	1.84	1.81	1.81	0.01	0.30/0.30	0.36/0.36	0.35/0.31
2.4	736	3581.79	1.83	1.84	1.82	1.76	1.75	0.01	0.27/0.27	0.43/0.43	0.32/0.28
2.5	913	3582.34	1.74	1.81	1.80	1.82	1.82	0.03	0.43/0.42	0.17/0.17	0.44/0.32
2.6	971	3582.57	1.87	1.79	1.79	1.78	1.77	0.01	0.43/0.41	0.22/0.22	0.35/0.34
2.7	1086	3583.16	1.64	1.91	1.90	1.77	1.77	0.08	0.33/0.33	0.26/0.26	0.37/0.32
2.8	1194/1195	3583.86	1.88	1.84	1.74	1.76	1.78	0.21	0.49/0.44	0.32/0.22	0.15/0.14
2.9	1200/1201	3583.91	1.88	1.76	1.76	1.81	1.78	0.12	0.54/0.42	0.21/0.16	0.30/0.22
2.10	1233/1234	3584.32	1.87	1.82	1.76	1.80	1.76	0.34	0.38/0.34	0.22/0.17	0.21/0.16
2.11	1252	3584.64	1.95	1.88	1.87	1.65	1.65	0.14	0.72/0.71	0.05/0.05	0.15/0.14
2.12	1259	3584.78	1.76	1.86	1.86	1.77	1.76	0.35	0.47/0.47	0.07/0.07	0.21/0.21
2.13	1268/1269	3585.03	1.81	1.77	1.77	1.87	1.78	0.21	0.60/0.53	0.16/0.11	0.16/0.18
2.14	1274	3585.07	1.91	1.79	1.65	1.86	1.78	0.26	0.60/0.58	0.08/0.08	0.15/0.14
2.15	1283	3585.28	1.71	1.89	1.88	1.77	1.76	0.52	0.38/0.38	0.08/0.08	0.14/0.14
2.16	1310/1311	3586.79 /3586.80	1.88	1.70	1.69	1.87	1.86	0.30	0.44/0.42	0.06/0.06	0.34/0.32
2.17	1328	3589.58	1.78	1.80	1.80	1.82	1.80	0.41	0.37/0.36	0.08/0.08	0.33/0.33

6.6 $[NpO_2]^{2+}$ Np $M_{4/5}$-Edge RAS(SD) XANES:

Figure S15 presents the simulated RAS(SD) Np M_5-edge XANES spectrum of $[NpO_2]^{2+}$ with a two peak profile consistent with experiment. Peak 1 contains a small shoulder with transitions labelled 1.1 - 1.4 in figure S16 which are assigned to core-transitions into the non-bonding 5f orbitals, followed by the set of transitions 1.5 – 1.12 under the main peak which correspond to core-excitations into the π^*_u orbitals. Across these transitions, σ^*_u occupancy ranges between 0.01 – 0.03 and is considered unoccupied. In comparison the second intense peak labelled 2, contains a large number of low intensity transitions which in combination generate the full XANES peak intensity. A selected sample of intense transitions labelled 2.1 – 2.5 are assigned to core-excitations into the σ^*_u. While occupation of the σ^*_u orbital is low, ranging from 0.08 – 0.12, these values are above the background level seen in transitions 1.1 - 1.12 and assignment of peak 2 to core-excitation into the σ^*_u would agree with transitions found at the RAS(S) level of simulation, were core-state multiconfigurational nature is less pronounced. To represent the overall assignment of peak 1, the highest intensity transition labelled 1.8 is chosen, and the corresponding degenerate pair of states for this transition are taken for additional covalency analysis. For peak 2, the highest intensity transition 2.5 is chosen out of those sampled and corresponds to the highest natural occupation of the σ^*_u out of the set at 0.12.

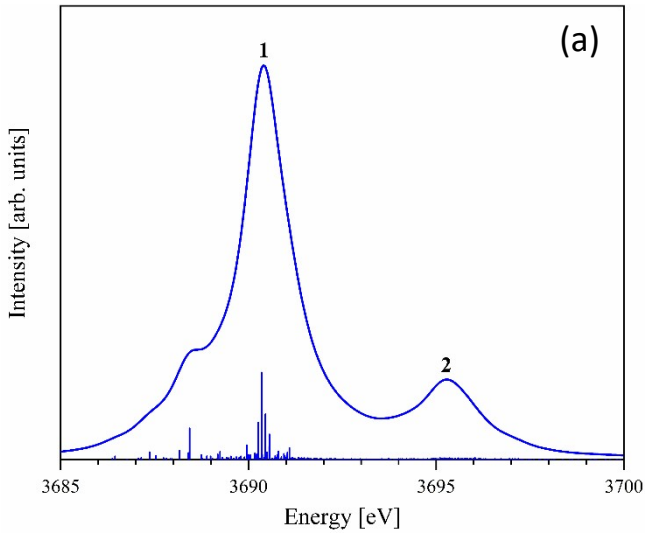

Figure S15: The theoretical RAS(SD) $[NpO_2]^{2+}$ Np M_5-edge XANES spectrum annotated with peak labels.

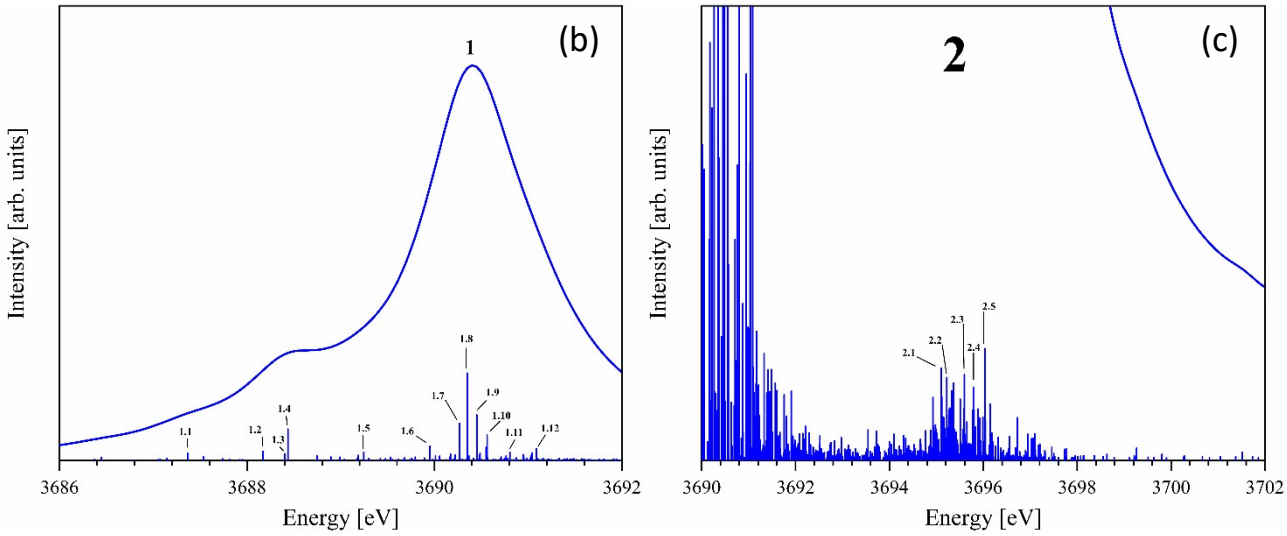

Figure S16: The theoretical RAS(SD) $[NpO_2]^{2+}$ Np M_5-edge XANES spectrum split into the two peak regions (a) 3686-3692 eV and (b) 3690 – 3702 eV. Spectra are annotated with peak and stick transition labels. Assignments of labelled transitions can be found in table S24.

Table S24: Assignments for M_5-edge XANES for $[NpO_2]^{2+}$ at the RAS(SD) level of theory. Table reports the natural populations of the spin-orbit natural orbitals for key core-states. Transitions correspond to assignments made in figures S15 and S16. States corresponds to the spin-orbit coupled state numbers assigned by the OpenMolcas RASSI calculation. Energy corresponds to the state energy in electron-volts.

Transition	State	Energy	3d	3d	3d	3d	3d	σu*	πu*	φu	δu
	GS	0	2.00	2.00	2.00	2.00	2.00	0.04	0.05/0.05	0.46/0.45	0.06/0.05
1.1	47/48	3687.37	1.97	1.86	1.86	1.65	1.65	0.01	0.03/0.03	0.52/0.51	0.48/0.48
1.2	91/92	3688.17	1.96	1.96	1.96	1.56	1.56	0.01	0.06/0.06	0.46/0.46	0.52/0.52
1.3	94/93	3688.40	1.86	1.85	1.83	1.83	1.64	0.01	0.10/0.10	0.28/0.28	0.65/0.65
1.4	95/96	3688.44	1.86	1.81	1.81	1.76	1.76	0.01	0.11/0.11	0.40/0.40	0.53/0.53
1.5	154/153	3689.25	1.90	1.89	1.75	1.75	1.71	0.02	0.31/0.31	0.49/0.49	0.26/0.26
1.6	236/235	3689.95	1.84	1.84	1.81	1.81	1.71	0.01	0.28/0.28	0.45/0.44	0.36/0.35
1.7	296/295	3690.27	1.78	1.71	1.70	1.91	1.91	0.03	0.36/0.36	0.39/0.38	0.41/0.40
1.8	309/310	3690.35	1.76	1.77	1.77	1.85	1.85	0.02	0.21/0.21	0.61/0.61	0.36/0.36
1.9	327/328	3690.45	1.85	1.84	1.79	1.79	1.72	0.02	0.30/0.32	0.43/0.42	0.40/0.40
1.10	352/351	3690.56	1.85	1.85	1.78	1.78	1.75	0.02	0.40/0.32	0.36/0.32	0.42/0.42
1.11	422/421	3690.80	1.84	1.84	1.81	1.76	1.75	0.02	0.35/0.33	0.37/0.37	0.55/0.53
1.12	502/501	3691.09	1.93	1.93	1.81	1.80	1.53	0.02	0.37/0.34	0.31/0.29	0.63/0.42
2.1	3716/3715	3695.10	1.81	1.80	1.80	1.80	1.78	0.08	0.48/0.48	0.52/0.52	0.45/0.43
2.2	3837/3838	3695.22	1.82	1.80	1.80	1.79	1.79	0.08	0.49/0.46	0.57/0.54	0.41/0.40
2.3	4193/4194	3695.60	1.81	1.80	1.80	1.80	1.80	0.07	0.57/0.55	0.47/0.46	0.43/0.41
2.4	4364/4363	3695.79	1.82	1.82	1.80	1.79	1.77	0.07	0.57/0.56	0.46/0.45	0.44/0.42
2.5	4557/4558	3696.03	1.84	1.83	1.78	1.78	1.77	0.12	0.51/0.50	0.46/0.45	0.44/0.44

7. Additional Theoretical Spectra & Assignments at the RAS(S) Level of Theory:

Due to the wavefunction constraints at the RAS(S) level, generated core-states will only involve electrons entering the RAS3 space from the core-orbitals in RAS1. This allows for a clear assignment of peaks to distinct core-excitations.

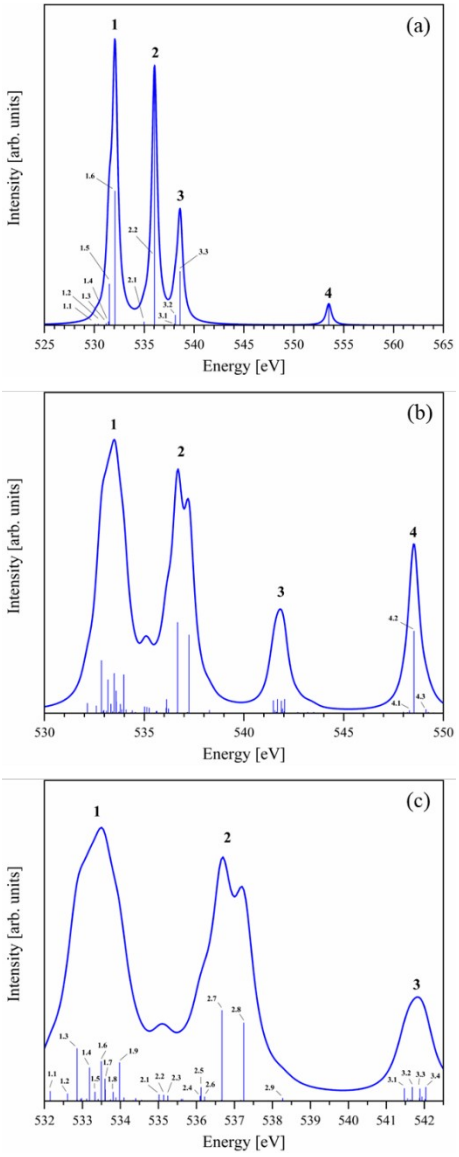

Figure S17: Theoretical RAS(S) oxygen K-edge XANES spectra for (a) $[UO_2]^{2+}$ and (b,c) $[NpO_2]^{2+}$. Spectra are annotated with peak and stick transition labels. Assignments for transitions can be found in tables S25 and S26.

7.1 $[UO_2]^{2+}$ O K-Edge RAS(S) XANES:

Figure S17(a) shows the simulated oxygen k-edge XANES for $[UO_2]^{2+}$ at the RAS(S) level of theory. Natural orbital occupations for core-excited states are contained in table S25. Peak 1 contains two intense transitions labelled 1.5 and 1.6, corresponding to core-excitations into π^*_u. Peak 2 contains an intense transition labelled 2.2 corresponding to a core-excitation into σ^*_u. Peak 3 contains two intense transitions labelled 3.2 and 3.3 corresponding to core-excitations into π^*_g. Finally peak 4 corresponds to a core-excitation into the σ^*_g orbital. A fourth peak is assigned to a core-excitation into the high energy σ^*_g orbital. A small shoulder is found to occur on peak 1, corresponds to transitions labelled 1.1- 1.3, which are core-excitations into the non-bonding 5f orbitals. Detailed assignments given in table S25.

Table S25: Assignments for $[UO_2]^{2+}$ oxygen K-edge XANES RAS(S) simulation. Table reports the natural populations of the spin-orbit natural orbitals for key core-states. Transitions correspond to assignments made in figure S17(a). States corresponds to the spin-orbit coupled state numbers assigned by the OpenMolcas RASSI calculation. Energy corresponds to the state energy in electron-volts.

Transition	State	Energy	1s(g)	1s(u)	σu*	πu*	πg*	σg*	φu	δu
1.1	4/5	530.08	1.00	2.00	0.00	0.00/0.00	0.00/0.00	0.00	0.08/0.08	0.80/0.04
1.2	7/8	530.40	1.00	2.00	0.00	0.00/0.00	0.00/0.00	0.00	0.39/0.34	0.22/0.05
1.3	14/15	531.19	1.00	2.00	0.00	0.00/0.00	0.00/0.00	0.00	0.60/0.33	0.06/0.01
1.4	19	531.42	1.10	1.90	0.01	0.44/0.44	0.05/0.05	0.00	0.00/0.00	0.00/0.00
1.5	20/21	531.51	1.10	1.90	0.03	0.65/0.22	0.08/0.02	0.00	0.00/0.00	0.00/0.00
1.6	24/25	532.08	1.09	1.91	0.00	0.67/0.19	0.07/0.02	0.00	0.00/0.00	0.04/0.01
2.1	27/28	534.98	1.05	1.95	0.93	0.01/0.01	0.00/0.00	0.05	0.00/0.00	0.00/0.00
2.2	29	536.03	0.05	1.95	0.95	0.00/0.00	0.00/0.00	0.04	0.00/0.00	0.00/0.00
3.1	31	538.03	1.88	1.12	0.00	0.06/0.06	0.44/0.44	0.00	0.00/0.00	0.00/0.00
3.2	32/33	538.12	1.89	1.11	0.00	0.09/0.01	0.75/0.15	0.00	0.00/0.00	0.00/0.00
3.3	36/37	538.60	1.91	1.09	0.00	0.08/0.02	0.76/0.14	0.00	0.00/0.00	0.00/0.00
4	41	553.51	1.96	1.04	0.04	0.00/0.00	0.00/0.00	0.96	0.00/0.00	0.00/0.00

7.2 $[NpO_2]^{2+}$ O K-Edge RAS(S) XANES:

The simulated oxygen k-edge XANES spectrum in figure S17(b) contains a four peak structure akin to that of $[UO_2]^{2+}$. In the ground-state of $[NpO_2]^{2+}$, a single unpaired electron occupies the non-bonding 5f orbitals. All core-excitations also retain this single electron, which continues to span the four non-bonding 5f orbitals, this is the case for all states labelled and characterized in Table S26. The additional electron occupying the set of non-bonding 5f orbitals generates an increased number of possible electronic configurations when compared to uranyl, thus it is not surprising that the XANES spectrum has a greater density of states contributing to each peak. This is clear to see in peaks 1 and 3 for example. Peaks 2 and 4 contain distinct high-intensity transitions labelled 2.7 and 2.8 for peak 2, and a single state labelled 4.2 for peak 4.

Transitions 2.7 and 2.8 are core-excitations into the σ^*_u orbital, and transition 4.2 corresponds to a core-excitation into the σ^*_g orbital. Transitions 4.1 and 4.3 are lower intensity core-excitations into the σ^*_g. A number of transitions contribute to peak 1, labelled from 1.3 – 1.9 in figure S17(b). All these core-excitations contain varying degrees of π^*_u occupation. Meaning an overall assignment to peak 1 can still be made, which corresponds to a core-excitation into the π^*_u orbital. Transitions labelled 1.2 and 1.3 present core-states with the majority of the excited electron from the core-1s orbitals residing across the non-bonding 5f orbitals, akin to the shoulder assigned in $[UO_2]^{2+}$. Between peaks 1 and 2, transitions labelled 2.1 to 2.3 are found to be intermediate states between the two main core-excitations into the π^*_u and σ^*_u. They contain remnants of π^*_u occupation but also additional occupation of the non-bonding 5f orbitals and σ^*_u to varying degrees depending on the state. Peak 3 contains a number of states that contribute to the overall peak. All four transitions labelled 3.1 – 3.4 contain clear core-excitations into the π^*_g orbital, allowing this peak to be ascribed to this core-excitation overall. On the whole, the peak assignments are characteristic of those made for $[UO_2]^{2+}$, indicating a similar energy order of the anti-bonding orbitals found in $[NpO_2]^{2+}$. Detailed assignments given in table S26.

Table S26: Assignments for $[NpO_2]^{2+}$ oxygen K-edge XANES RAS(S) simulation. Table reports the natural populations of the spin-orbit natural orbitals for key core-states. Transitions correspond to assignments made in figure S17(b). States corresponds to the spin-orbit coupled state numbers assigned by the OpenMolcas RASSI calculation. Energy corresponds to the state energy in electron-volts.

Transition	State	Energy	1s(g)	1s(u)	σu*	πu*	πg*	σg*	φu	δu
1.1	28/27	532.15	1.01	1.99	0.00	0.05/0.05	0.00/0.00	0.00	0.47/0.47	0.50/0.46
1.2	33/34	532.61	1.04	1.96	0.02	0.20/0.20	0.02/0.02	0.00	0.24/0.24	0.55/0.51
1.3	37/38	532.89	1.09	1.91	0.05	0.40/0.40	0.04/0.04	0.00	0.44/0.44	0.09/0.09
1.4	50/49	533.19	1.09	1.91	0.06	0.38/0.38	0.04/0.04	0.01	0.33/0.33	0.25/0.19
1.5	53/54	533.33	1.03	1.97	0.02	0.15/0.15	0.02/0.02	0.00	0.21/0.21	0.63/0.60
1.6	59/60	533.50	1.08	1.92	0.01	0.36/0.36	0.04/0.04	0.00	0.22/0.22	0.39/0.35
1.7	62/61	533.59	1.10	1.90	0.02	0.44/0.43	0.05/0.05	0.00	0.22/0.22	0.37/0.20
1.8	79/80	533.81	1.06	1.94	0.04	0.26/0.26	0.03/0.03	0.00	0.37/0.27	0.37/0.37
1.9	87/88	533.97	1.06	1.94	0.04	0.26/0.26	0.03/0.03	0.00	0.31/0.27	0.40/0.40
2.1	122/121	535.01	1.07	1.93	0.09	0.22/0.22	0.03/0.03	0.01	0.27/0.26	0.45/0.42
2.2	131/132	535.14	1.09	1.91	0.20	0.34/0.34	0.03/0.03	0.02	0.19/0.19	0.40/0.26
2.3	139/140	535.25	1.06	1.94	0.04	0.15/0.15	0.03/0.03	0.00	0.24/0.23	0.65/0.48
2.4	153/154	536.10	1.11	1.89	0.72	0.12/0.12	0.02/0.02	0.08	0.41/0.41	0.07/0.04
2.5	156/155	536.12	1.10	1.90	0.69	0.13/0.13	0.02/0.02	0.07	0.40/0.40	0.12/0.04
2.6	159/160	536.21	1.10	1.90	0.57	0.15/0.15	0.02/0.02	0.06	0.34/0.34	0.23/0.12
2.7	165/166	536.67	1.09	1.91	0.85	0.03/0.03	0.00/0.00	0.08	0.47/0.46	0.05/0.02
2.8	175/176	537.25	1.10	1.90	0.71	0.10/0.10	0.02/0.02	0.07	0.39/0.39	0.14/0.08
2.9	187/188	538.27	1.09	1.91	0.82	0.08/0.08	0.01/0.01	0.07	0.03/0.03	0.49/0.37
3.1	209/210	541.47	1.90	1.10	0.00	0.05/0.05	0.45/0.45	0.00	0.33/0.32	0.26/0.08
3.2	220/219	541.68	1.89	1.11	0.00	0.06/0.06	0.44/0.44	0.01	0.26/0.26	0.25/0.22
3.3	225/226	541.88	1.89	1.11	0.00	0.07/0.07	0.45/0.45	0.00	0.19/0.19	0.32/0.26
3.4	234/233	542.04	1.91	1.09	0.00	0.12/0.10	0.47/0.44	0.00	0.35/0.34	0.10/0.08
4.1	326/325	548.30	1.89	1.11	0.11	0.01/0.01	0.02/0.02	0.88	0.06/0.06	0.59/0.26
4.2	331/332	548.53	1.92	1.08	0.08	0.00/0.00	0.01/0.01	0.91	0.41/0.41	0.11/0.07
4.3	342/341	549.13	1.90	1.10	0.09	0.00/0.00	0.00/0.00	0.90	0.39/0.39	0.17/0.05

7.3 RAS(S) Assignments for Simulated Uranium $M_{4/5}$-edge XANES:

Figure S18 shows the spin-orbit splitting between the M_5- and M_4-edges for both systems.

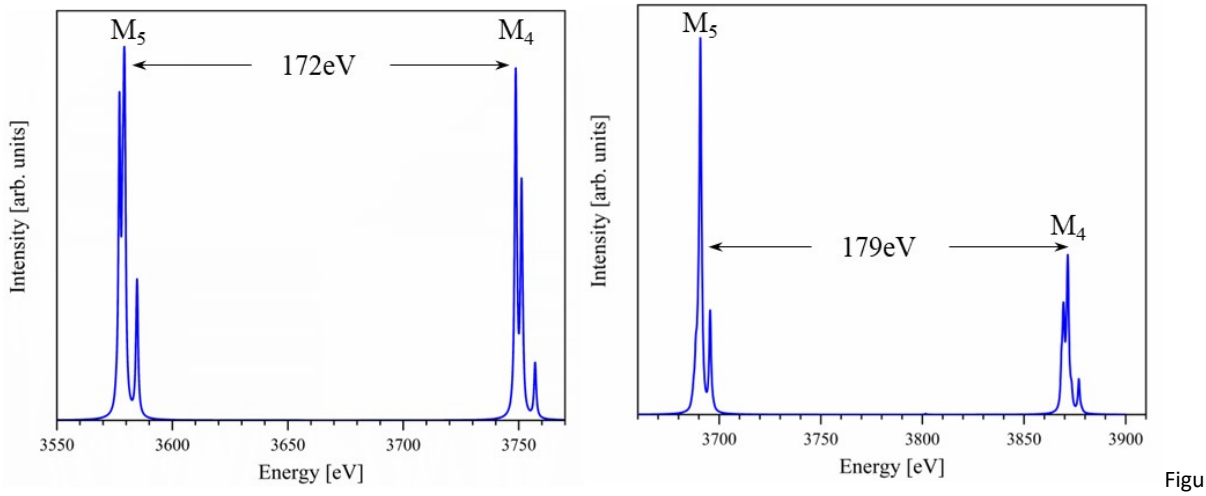

Figure S18: Spin-orbit coupling splitting values between the An M_5- and M_4-edges for $[UO_2]^{2+}$ and $[NpO_2]^{2+}$ at the RAS(S) level of theory.

7.4 $[UO_2]^{2+}$ U $M_{4/5}$-Edge RAS(S) XANES:

The simulated U M_4-edge spectrum of $[UO_2]^{2+}$ is labelled in figure S19(a). The spectrum consists of a three-peak structure (peaks 1-3) in agreement with experiment.[2] Full natural orbital occupations for labelled transitions are contained within Table S27. Peak 1 contains four labelled transitions which can be assigned to core-excitations into the non-bonding 5f orbitals. Peak 2 contains five labelled transitions which can all be assigned to core-excitations into the π^*_u orbitals, and peak 3 contains three transitions which can be assigned to core-excitations into the σ^*_u orbital. These assignments agree with those made by Vitova *et al*.[2]

The simulated U M_5-edge Spectrum of $[UO_2]^{2+}$ was also generated and labelled in figure S19(b). The spectrum has a three-peak structure, with a potential shoulder on the first peak. Peak 1 consists of two high intensity transitions labelled 1.2 and 1.3, each corresponding to core-excitations into the non-bonding 5f orbitals. A low intensity transition labelled 1.1 also corresponds to a core-excitation into the non-bonding 5f orbitals. Peak 2 contains four states labelled 2.1 – 2.4, each assigned to core-excitations into the π^*_u orbitals. Peak 3 contains three labelled transitions from 3.1 – 3.3, each assigned to clear core-excitations into the σ^*_u orbital. Detailed assignments given in table S28.

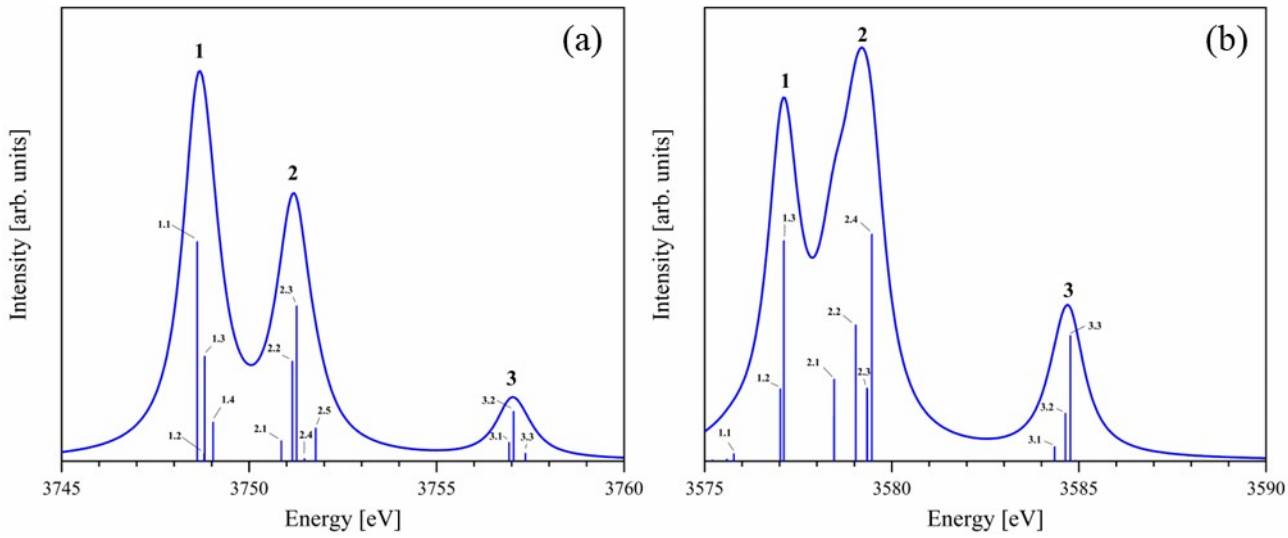

Figure S19: $[UO_2]^{2+}$ U $M_{4/5}$-edge XANES RAS(S) simulated spectra showing the (a) M_4-edge and (b) M_5-edge spectra. Peak and stick transition labels for the M_4-edge and M_5-edges are also presented. Assignments can be found in tables S27 and S28.

Table S27: Assignments for M_4-edge XANES for $[UO_2]^{2+}$ at the RAS(S) level of theory. Table reports the natural populations of the spin-orbit natural orbitals for key core-states. Transitions correspond to assignments made in figure S19(a). States corresponds to the spin-orbit coupled state numbers assigned by the OpenMolcas RASSI calculation. Energy corresponds to the state energy in electron-volts.

Transition	State	Energy	3d	3d	3d	3d	3d	σu*	πu*	φu	δu
1.1	101/102	3748.62	1.87	1.73	1.73	1.85	1.82	0.00	0.01/0.00	0.36/0.33	0.22/0.09
1.2	107/108	3748.80	1.62	1.98	1.95	1.81	1.64	0.00	0.00/0.00	0.44/0.42	0.10/0.04
1.3	109	3748.81	2.00	1.60	1.60	1.90	1.90	0.00	0.00/0.01	0.00/0.00	0.50/0.49
1.4	114/115	3749.04	1.98	1.63	1.62	1.90	1.88	0.00	0.01/0.00	0.00/0.00	0.50/0.48
2.1	119/120	3750.86	1.60	2.00	1.97	1.79	1.63	0.01	0.76/0.22	0.00/0.00	0.01/0.00
2.2	121/122	3751.15	1.69	1.80	1.70	1.91	1.89	0.00	0.74/0.25	0.01/0.00	0.00/0.00
2.3	125	3751.26	1.61	2.00	2.00	1.70	1.70	0.00	0.51/0.48	0.00/0.00	0.00/0.00
2.4	128/129	3751.48	1.77	1.83	1.81	1.82	1.77	0.01	0.57/0.42	0.00/0.00	0.00/0.00
2.5	133	3751.78	2.00	1.60	1.60	1.90	1.90	0.00	0.50/0.50	0.00/0.00	0.00/0.00
3.1	135/136	3756.93	1.60	2.00	2.00	1.72	1.68	0.99	0.01/0.00	0.00/0.00	0.00/0.00
3.2	137	3757.06	1.60	2.00	2.00	1.70	1.70	1.00	0.00/0.00	0.00/0.00	0.00/0.00
3.3	139/140	3757.37	2.00	1.60	1.60	1.92	1.88	0.99	0.00/0.00	0.00/0.00	0.00/0.00

Table S28: Assignments for M_5-edge XANES for $[UO_2]^{2+}$ at the RAS(S) level of theory. Table reports the natural populations of the spin-orbit natural orbitals for key core-states. Transitions correspond to assignments made in figure S19(b). States corresponds to the spin-orbit coupled state numbers assigned by the OpenMolcas RASSI calculation. Energy corresponds to the state energy in electron-volts.

Transition	State	Energy	3d	3d	3d	3d	3d	σu*	πu*	φu	δu
1.1	21	3575.78	2.00	1.79	1.79	1.71	1.71	0.00	0.01/0.01	0.14/0.14	0.35/0.35
1.2	47	3577.02	1.98	1.53	1.52	1.98	1.98	0.00	0.02/0.02	0.02/0.02	0.46/0.45
1.3	48/49	3577.12	1.90	1.71	1.71	1.85	1.82	0.00	0.12/0.01	0.30/0.30	0.14/0.13
2.1	56/57	3578.46	1.63	1.94	1.98	1.98	1.48	0.02	0.59/0.34	0.02/0.02	0.01/0.00
2.2	67/68	3579.04	1.46	1.94	1.76	1.99	1.84	0.00	0.73/0.19	0.01/0.01	0.03/0.02
2.3	71/72	3579.34	2.00	1.52	1.51	1.99	1.98	0.00	0.51/0.47	0.00/0.00	0.01/0.01
2.4	73	3579.47	1.98	1.91	1.88	1.62	1.62	0.01	0.47/0.47	0.00/0.00	0.03/0.03
3.1	75/76	3584.35	1.41	2.00	2.00	1.89	1.70	0.99	0.01/0.00	0.00/0.00	0.00/0.00
3.2	79/80	3584.64	2.00	1.95	1.83	1.70	1.52	0.99	0.01/0.01	0.00/0.00	0.00/0.00
3.3	81	3584.78	1.40	2.00	2.00	1.80	1.80	0.97	0.01/0.01	0.00/0.00	0.00/0.00

7.5 $[NpO_2]^{2+}$ Np $M_{4/5}$-Edge RAS(S) XANES:

The simulated Np M_5-edge spectrum of $[NpO_2]^{2+}$ is shown in figure S20(b). The spectrum reproduces the two-peak structure expected from experiment, but with the addition of a shoulder on peak 1. Additional plots Figure S20(e) and S20(f) show the labelled transitions under peaks 1 and 2 respectively. The highest intensity transition under peak 1 is labelled 1.9 and can be assigned to a core-excitation into π^*_u orbitals. Lower intensity transitions (1.4 – 1.12) either side of 1.9 can also be assigned to core-excitations into the π^*_u orbitals with varying degrees of natural occupations. Smaller intensity transitions under the shoulder on peak 1, labelled 1.1 – 1.3, correspond to core-excitations into the non-bonding 5f orbitals. In simulation, we find that the core-excitations into the non-bonding 5f orbitals and into the π^*_u are energetically separable, with the core-states involving the non-bonding 5f orbitals coming first, followed by those states of higher intensity for the main peak into the π^*_u. Peak 2 has four labelled transitions 2.1 – 2.4, all corresponding to core-excitations into the σ^*_u orbital. Detailed assignments are given in table S29.

The simulated Np M_4-edge spectrum of $[NpO_2]^{2+}$ was also generated and labelled in figure S20(a). The spectrum consists of a three-peak structure, with a select number of states labelled in additional plots in figure S20(c) and S20(d). Peak 1 contains several transitions labelled 1.1 – 1.7. These states are assigned to core-excitations into the non-bonding 5f

orbitals. Peak 2 contains a high intensity transition labelled 2.5 for a core-excitation into the π^*_u orbitals. Additional density of states is present either side of this main excitation with varying degrees of π^*_u orbital occupation. Peak 3 contains a number of transitions labelled 3.1 – 3.5 which all correspond to core-excitations into the σ^*_u orbital. Detailed assignments are given in table S30.

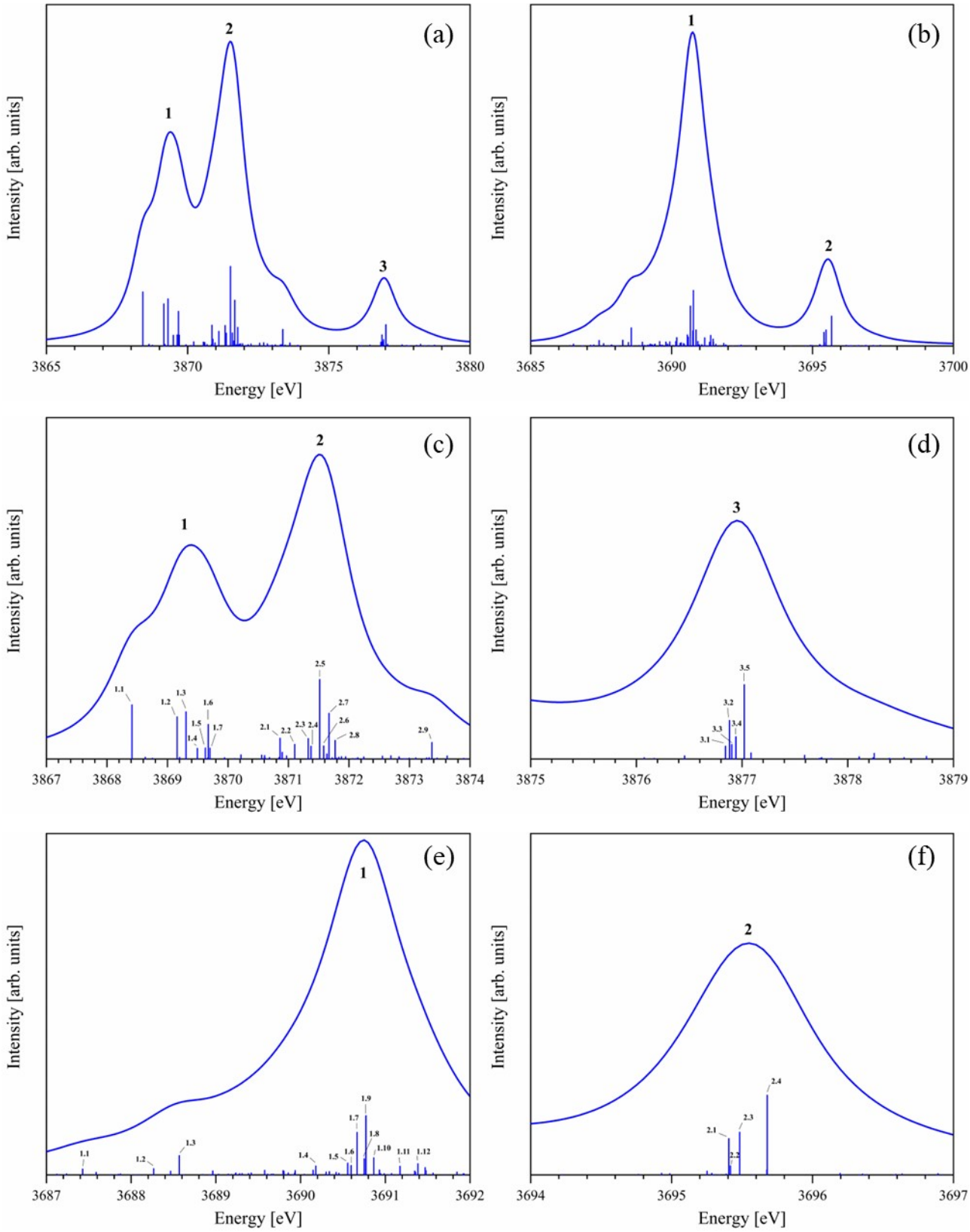

Figure S20: $[NpO_2]^{2+}$ Np $M_{4/5}$-edge XANES RAS(S) simulated spectra showing the (a) M_4-edge and (b) M_5-edge spectra. Peak and stick transition labels for the (b,c) M_4-edge and (e,f) M_5-edges are also presented. Assignments can be found in tables S29 and S30.

Table S29: Assignments for M_5-edge XANES for $[NpO_2]^{2+}$ at the RAS(S) level of theory. Table reports the natural populations of the spin-orbit natural orbitals for key core-states. Transitions correspond to assignments made in figure S20. States corresponds to the spin-orbit coupled state numbers assigned by the OpenMolcas RASSI calculation. Energy corresponds to the state energy in electron-volts.

Transition	State	Energy	3d	3d	3d	3d	3d	σu*	πu*	φu	δu
1.1	47/48	3687.43	1.97	1.87	1.86	1.65	1.65	0.00	0.01/0.01	0.51/0.51	0.48/0.48
1.2	91/92	3688.27	1.98	1.55	1.55	1.96	1.96	0.00	0.05/0.04	0.44/0.44	0.52/0.52
1.3	96/95	3688.57	1.87	1.81	1.81	1.76	1.76	0.00	0.08/0.08	0.35/0.35	0.57/
1.4	217/218	3690.18	1.69	1.83	1.81	1.83	1.83	0.00	0.29/0.29	0.43/0.43	0.30/0.25
1.5	243/244	3690.56	1.87	1.89	1.88	1.68	1.68	0.01	0.38/0.37	0.26/0.26	0.35/0.35
1.6	247/248	3690.60	1.83	1.91	1.91	1.68	1.68	0.01	0.47/0.47	0.12/0.12	0.42/0.38
1.7	249/250	3690.67	1.84	1.86	1.86	1.72	1.72	0.01	0.37/0.36	0.27/0.27	0.37/0.35
1.8	255/256	3690.75	1.89	1.71	1.71	1.85	1.85	0.01	0.27/0.27	0.38/0.38	0.36/0.34
1.9	258/259/257/260	3690.77	1.85	1.73	1.73	1.85	1.84	0.01	0.35/0.19	0.48/0.48	0.26/0.25
1.10	263/264	3690.86	1.56	1.93	1.93	1.79	1.79	0.00	0.44/0.44	0.33/0.33	0.21/0.22
1.11	294/293	3691.17	1.73	1.77	1.78	1.90	1.83	0.01	0.44/0.36	0.35/0.34	0.25/0.24
1.12	315/316	3691.39	1.47	1.98	1.98	1.79	1.78	0.01	0.42/0.39	0.40/0.39	0.19/0.19
2.1	408/407	3695.41	1.80	1.86	1.84	1.76	1.74	0.93	0.06/0.06	0.44/0.44	0.04/0.04
2.2	410/409	3695.42	1.95	1.62	1.61	1.91	1.91	0.82	0.17/0.17	0.39/0.38	0.04/0.03
2.3	411/412	3695.48	1.85	1.92	1.89	1.68	1.65	0.93	0.05/0.05	0.45/0.44	0.04/0.04
2.4	419/420	3695.68	1.47	1.97	1.97	1.80	1.80	0.90	0.08/0.08	0.43/0.43	0.04/0.04

Table S30: Assignments for M_4-edge XANES for $[NpO_2]^{2+}$ at the RAS(S) level of theory. Table reports the natural populations of the spin-orbit natural orbitals for key core-states. Transitions correspond to assignments made in figure S20. States corresponds to the spin-orbit coupled state numbers assigned by the OpenMolcas RASSI calculation. Energy corresponds to the state energy in electron-volts.

Transition	State	Energy	3d	3d	3d	3d	3d	σu*	πu*	φu	δu
1.1	505/506	3868.42	1.61	2.00	2.00	1.70	1.70	0.00	0.01/0.01	0.49/0.48	0.51/0.50
1.2	521/522	3869.16	1.97	1.63	1.63	1.89	1.89	0.00	0.03/0.03	0.42/0.41	0.56/0.55
1.3	527/528	3869.31	1.76	1.85	1.85	1.78	1.77	0.00	0.02/0.02	0.39/0.39	0.59/0.58
1.4	534/533	3869.50	1.96	1.64	1.64	1.88	1.88	0.00	0.02/0.02	0.48/0.48	0.50/0.50
1.5	541/542	3869.63	1.68	1.92	1.92	1.75	1.73	0.00	0.04/0.04	0.47/0.46	0.63/0.36
1.6	547/548	3869.67	1.66	1.94	1.94	1.73	1.73	0.00	0.04/0.04	0.46/0.46	0.54/0.46
1.7	549/550	3869.70	1.88	1.72	1.72	1.84	1.84	0.00	0.03/0.03	0.45/0.45	0.52/0.52
2.1	582/581	3870.86	1.64	1.96	1.96	1.72	1.72	0.01	0.48/0.48	0.44/0.43	0.08/0.08
2.2	594/593	3871.10	1.63	1.97	1.97	1.72	1.71	0.01	0.43/0.43	0.49/0.48	0.08/0.07
2.3	604/603	3871.33	1.90	1.70	1.70	1.85	1.85	0.01	0.48/0.48	0.46/0.46	0.06/0.06
2.4	607/608	3871.37	1.68	1.92	1.92	1.74	1.74	0.00	0.17/0.17	0.56/0.56	0.29/0.27
2.5	616/615	3871.52	1.64	1.96	1.96	1.72	1.72	0.00	0.47/0.46	0.41/0.40	0.13/0.12
2.6	618/617	3871.58	1.79	1.82	1.82	1.79	1.79	0.01	0.36/0.36	0.30/0.30	0.34/0.33
2.7	627/628	3871.67	1.72	1.88	1.88	1.76	1.76	0.00	0.36/0.36	0.47/0.48	0.15/0.18
2.8	635/636	3871.77	1.96	1.64	1.64	1.88	1.88	0.00	0.48/0.48	0.49/0.48	0.04/0.03
2.9	726/725	3873.37	1.86	1.74	1.74	1.83	1.83	0.00	0.25/0.25	0.31/0.31	0.44/0.44
3.1	760/759	3876.84	1.62	1.98	1.98	1.71	1.71	0.96	0.03/0.03	0.48/0.42	0.04/0.04
3.2	761/762	3876.88	1.60	2.00	2.00	1.70	1.70	0.98	0.01/0.01	0.48/0.45	0.03/0.03
3.3	764/763	3876.90	1.69	1.91	1.91	1.75	1.74	0.96	0.03/0.03	0.45/0.44	0.05/0.04
3.4	766/765	3876.94	1.93	1.67	1.67	1.87	1.87	0.75	0.24/0.24	0.34/0.34	0.04/0.04
3.5	769/770	3877.02	1.61	1.99	1.99	1.73	1.68	0.98	0.01/0.01	0.46/0.45	0.05/0.04

8. References:

1 R. G. Denning, J. C. Green, T. E. Hutchings, C. Dallera, A. Tagliaferri, K. Giarda, N. B. Brookes and L. Braicovich, *J Chem Phys*, 2002, **117**, 8008–8020.

2 T. Vitova, I. Pidchenko, D. Fellhauer, P. S. Bagus, Y. Joly, T. Pruessmann, S. Bahl, E. Gonzalez-Robles, J. Rothe, M. Altmaier, M. A. Denecke and H. Geckeis, *Nat Commun*, 2017, **8**, 16053.

3 R. Polly, B. Schacherl, J. Rothe and T. Vitova, *Inorg Chem*, 2021, **60**, 18764–18776.